University of Southern Queensland

Faculty of Engineering and Surveying

INVESTIGATION OF SOLAR THERMAL ENERGY ALTERNATIVES AND THEIR APPLICATIONS TO WATER HEATING AND AIR COOLING IN THE MEAT PROCESSING INDUSTRY

A dissertation submitted by

Zach Anthony Muller

in fulfillment of the requirements of

Courses ENG4111 and ENG4112

towards the degree of

Bachelor of Engineering (Mechanical)

Submitted: October, 2010

Abstract

This research project sought to provide insight into the possible applications of solar thermal energy within the meat processing industry..

This project is carried out in conjunction with Churchill Abattoir; with the view to develop a solar thermal alternative for producing heated water to cater in part for the needs of their operation whilst simultaneously providing refrigeration. In terms of an industry comparison, Churchill Abattoir is ranked approximately 25-30th of 180 abattoirs nationwide and processes (i.e. slaughter, bone and butcher) around 2500 cattle per week.

The meat processing industry has a high demand for heated water. Its uses vary from hand washing and laundry (≅43°C) to sterilisation of equipment such as saws, meat hooks knives etc (>83°C). It also has high energy needs for refrigeration.

A solar thermal system that could reduce energy costs in these areas would not only benefit Churchill Abattoir but may see further application within industry.

Project aims include

- Research current alternatives in solar thermal systems.
- Establish design parameters.
- Produce a conceptual solar thermal system.
- Investigate the potential of such a system to cooling processes.

The project began by researching the existing alternatives for system components such as energy collectors, solar tracking, chillers and heaters. Once the component variables and design parameters for a conceptual system had been established an initial design was proposed and analysed to determine its capabilities. As a result of the analysis components and sizes were selected for a real system that could be implemented at the abattoir.

This project seeks ultimately to improve abattoir operations by reducing non-renewable energy use through the development of a solar thermal system. Its outcomes have the potential to benefit the wider industry.

ENG4111 & ENG4112 Research Project

Limitations of Use

The Council of University of Southern Queensland, it's Faculty of Engineering and Surveying, and the staff of the University of Southern Queensland, do not accept any responsibility for the truth, accuracy or completeness of the material contained within or associated with this dissertation.

Persons using all or any part of this material do so at their own risk, and not at the risk of the Council of the University of Southern Queensland, its faculty of Engineering and Surveying or the staff of the University of Southern Queensland.

This dissertation reports an educational exercise and has no purpose or validity beyond this exercise. The sole purpose of the course "Project and Dissertation" is to contribute to the overall education within the students chosen degree program. This document, the associated hardware, software, drawings, and other material set out in the associated appendices should not be used for any other purpose: if they are used it is entirely at the risk of the user.

Prof Frank Bullen
Dean
Faculty of Engineering and Surveying

Certification

I certify that the ideas, designs and experimental work, results, analyses and conclusions set out in this dissertation are entirely my own effort except where otherwise indicated and acknowledged.

I further certify that the work is original and has not been previously submitted for assessment in any other course or institution, except where specifically stated.

Zach Muller

Student Number: 0050072640

Signature

Date

Acknowledgements

This project was carried out under the supervision of Steven Goh.

The project was carried out in conjunction with Churchill Abattoir, Ipswich. Many thanks are due to Mike Spence and Ben Blemmings for providing the site specific details used in the project.

Throughout the course of the project consultation with industry became necessary. I understand that they all had their own workloads and at times there were delays in assistance. However the work produced in this dissertation would not have been possible without their invaluable input.

Many thanks to:

Johan Dreyer, CEO of NEP Solar; for his advice regarding my yield analysis model, providing a clearer understanding regarding the design of parabolic trough systems & providing the results of their own their own analysis for comparison.

Shaun McKinnon, Business Development Manager at ECS Brisbane; for providing information on BROAD Absorption Chillers used in the final design.

Ray Findlay, Applications Engineer at Actrol Parts Salisbury and Claes Larsson of SWEP heat exchangers. I was very impressed with the assistance and speed of service provided by these two in the initial sizing/redesigning of heat exchange systems in the last days of the project. 3 days from start to finish!

Table of Contents

List of Figures

List of Tables

Nomenclature

A_a	Aperture area	m^2
A_r	Receiver area	m^2
α	Solar altitude angle	degrees
β	Collector tilt angle	degrees
C	Concentration ratio	
c_p	Specific heat	kJ/kg
δ	Declination angle	degrees
η	Collector efficiency	
η_o	Optical efficiency	
FF	Wind speed	m/s
F_R	Heat removal factor	
γ	Optical intercept factor	
h	Hour angle	degrees
$\bar{H}$	Monthly average total insolation on a horizontal terrestrial surface	MJ/m^2
$\bar{H}_D$	Monthly average daily diffuse insolation on a horizontal terrestrial surface	MJ/m^2-d
$\bar{H}_o$	Monthly average daily total insolation on a horizontal	MJ/m^2-d

	extraterrestrial surface	
θ	Incidence angle	degrees
$\bar{K}_T$	Monthly average clearness index	
K_θ	Incidence angle modifier	
p	Solar profile angle	degrees
ρ	Trough reflectance	
Q_u	Energy collected	kW
r_d	Ratio of hourly diffuse radiation to daily diffuse radiation	
r	Ratio of hourly total radiation to daily total radiation	
RH	Relative humidity	
T_a	Ambient temperature	°C
T_i	Fluid temperature into collector	°C
τ	Transmittance	
U_o	Overall heat loss coefficient	W/m^2-K
ϕ	Solar zenith	degrees
z	Solar azimuth angle	degrees

Chapter 1 - Introduction

1.1 Outline

This research has provided insight into the possible applications of solar thermal energy within the meat processing industry. A conceptual system was designed and subsequently analysed in order to determine whether it would be possible to provide for the water heating needs of the abattoir whilst simultaneously cooling air for refrigeration.

1.2 Background

This project is carried out in conjunction with Churchill Abattoir (located in western Ipswich, Queensland) with the view to develop a solar thermal alternative to producing heated water for their operation. In terms of industry comparison, Churchill Abattoir is ranked approximately 25-30th of 180 abattoirs nationwide and processes (i.e. slaughter, bone and butcher) around 2500 cattle per week. They supply Woolworths directly with cleaned carcasses. Woolworths lease a building onsite known as the "boning room" from Churchill Abattoir. Woolworths must purchase utilities from Churchill that they themselves do not produce i.e. hot water and refrigeration.

The meat processing industry has a high demand for heated water. Its uses vary from hand washing and laundry (≅43°C) to sterilisation of equipment such as saws, meat hooks knives etc (>83°C). In 2008, the boning room alone used 9ML and 11ML of hot and warm water respectively.

Many abattoirs produce their own hot water as a by-product of some other process. For example, Churchill Abattoir uses an 8 MW coal fired boiler to produce steam to

drive a "cooker" that renders meat by-products for further use. At the same time some of this steam is passed through a heat exchanger that heats water for use in the plant. Over one year the plant uses approximately 150 ML of water with a coal bill of $100,000.

Refrigeration at the abattoir is provided through utilization of 5 x Mycom™ compressors coupled to 12 cooling towers/chillers provide cooling to the abattoir and the boning room. The working fluid is Anhydrous Ammonia which, at fluid temperatures of -9°C to -5°C. The cold rooms are maintained at approximately 4°C although the acceptable range is 2°C to 10°C. As fresh carcasses are brought into the cold rooms there is a sudden "heat shock" so to speak and the refrigeration system must deal with this sudden dramatic temperature increase.

Churchill Abattoir approached the University of Southern Queensland with the project proposal for the conceptual design of a solar thermal system that would not only be capable of producing heated water but would also have the ability to provide air cooling. A solar thermal system that would provide water at the temperature and flow rates required by the abattoir or the boning room would be incredibly expensive both in terms of installation and space requirements, not to mention that a solar thermal cooling system could never match the minimum temperature achievable by traditional refrigeration. Rather it was envisaged that the system would not be a sole solution to the energy needs but rather a renewable energy "boost" system with the aim to reduce overall energy consumption.

1.3 Aim

This research aimed to investigate current solar thermal technology with the intention of designing a conceptual system that would provide for the water heating needs of a typical abattoir whilst simultaneously having some application to cooling air for boosting refrigeration. In recent years there has been an increase in the use of

solar thermal energy, especially in the domestic sector and consequently there is a wealth of information system design for such needs. However there is a far greater potential for energy savings through the development of solar thermal systems for use in the industrial sector. At present the majority of large scale solar thermal systems are designed for power generation, not water heating. This project arose from the need to further this area of solar thermal system design.

1.4 Objectives

The objective of this research was to determine if a solar thermal system could be designed such that it would provide for the water heating needs of a medium scale abattoir whilst also having the potential to cool air to provide a refrigeration boost. After examining available collection, storage and cooling technologies and defining the design parameters, various systems were proposed. The design deemed to have best satisfied these requirements was then completely analysed in order to fully determine its capabilities and limitations.

1.5 Summary

This dissertation aims to provide a solar thermal water heating system to satisfy the usage needs of a mid-sized abattoir; i.e. industrial scale. Due to its specific application to the meat processing industry it furthers engineering knowledge in this field. In designing this system a great deal of literature was drawn upon in determining the current solar thermal technologies available. The next chapter presents a review of this technology in terms of energy collection, solar tracking, system design, heat storage and air cooling. Chapter 3 identifies the design parameters, selection process and means of system analysis. The potential designs,

individual analysis is carried out in Chapter 4. The conclusions drawn from this research are presented in Chapter 5

Chapter 2 – Initial Research

2.1 Introduction

In recent years the popularity of renewable energy has risen dramatically. Increased awareness of the environmental impacts surrounding many current practices has seen both industry and consumers changing their practices; further encouraged by government grants to do so.

Consequently there are vast amounts of basic information available on solar thermal system concepts. This chapter seeks to establish the current state of solar thermal technology as applied to water heating/air cooling on an industrial scale. It also serves to inform the reader of the variables available regarding energy collection, system design and cooling that are ultimately selected from to produce conceptual designs.

Please note that the following literature review presents a lot of fundamental information relating to collector types, solar theory and analysis methods. Consequently much of the material is referenced to a few texts whose guidance was used extensively. Sources that support these findings but may not have been referenced in text are presented in a bibliography at the end of the document.

2.2 Collecting Solar Thermal Energy

Solar collectors are devices that absorb solar energy and pass it on to some heat transfer fluid (air, water oil etc). The heat within the HTF may then be used directly or transferred to a storage medium from which energy can be drawn during inadequate insolation.

Collecting devices themselves can be classified primarily by their type, concentrating or non-concentrating. In non-concentrating systems, collection area is equal to absorption area. The second design feature used for grouping designs is whether they are stationary or sun tracking. Sun tracking systems may operate on one or two axis rotation. A solar collector achieves the greatest energy density when solar radiation strikes it normal to its inclination. Through sun tracking this feature can be exploited for a greater time period though they add substantial cost to system design.

The following is an outline that provides a general description of the design and capabilities of collectors available in today's marketplace. The information is generic and is provided a preface to the engineering project.

Stationary, Non-Concentrating Collectors

Note that whilst the collectors outlined in the following section are typically produced to be non-concentrating, one can install reflectors around them to focus radiation onto them for better operation. However here they are referred to in their basic form. Non concentrating collectors can utilise all forms (beam, diffuse and ground reflected) of solar radiation.

2.2.1 Flat Plate Collectors

A typical flat plate collector is shown below.

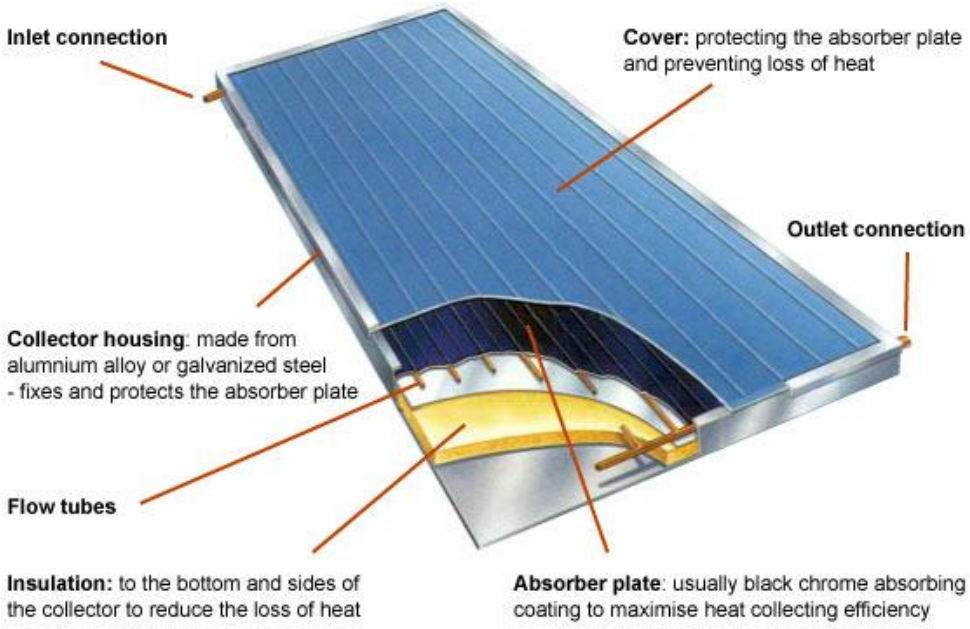

Figure 2.1 A typical flat plate collector, (Source: GreenSpec, 2010)

As these collectors are most commonly used for domestic water heating there is vast amounts of information regarding their construction. A typical flat plate collector consists of 5 components:

- A cover – one or more sheets of glass/radiation transmitting material. Glass is most commonly used as it can transmit up to 90% of the incoming shortwave radiation whilst trapping practically all of the longwave radiation emitted by the absorber plate (Kalogiru, 2009).

- Fluid passages – tubes, fins or piping that carry the heat transfer fluid through the system. Heat absorbed by the plate is conducted to the working fluid and piped away.

- Absorber plate – Grooved, corrugated or flat plates to which the fluid passages attach. Plates are commonly shaped to allow embedding of the passages. Absorber plates typically receive a selective coating: i.e. one that allows high absorption of short wave radiation (solar influx) whilst maintaining low emittance to limit re-radiation.

- Headers – inlet and outlet piping.

- Insulation – minimizing heat lost from the back of the collector.

Radiation passes through the cover and into the collector where its energy is transferred as heat to the absorber plate. As fluid passes through the flow tubes it is heated. It follows that the outlet temperature is directly related to the mass flow rate of the fluid through the system. That is to say that slower flow leads to higher temperatures. This goes on until there is no flow and stagnation temperature is reached. At stagnation temperature, heat transferred to the fluid is equal to the system losses and so temperature stabilizes. This concept holds for any collector.

FPC's are usually a fixed installation with no tracking. They should be oriented toward the equator; that is facing north in southern hemisphere and vice versa. According to Kalogiru (2004) the angle of tilt is approximately equal to the latitude.

Kalogiru (2009 p.122) states that FPC's are capable of temperatures of up to 80°C. They are capable of utilizing both direct and diffuse (scattered by atmosphere) radiation and their performance suffers greatly during cloudy weather.

An FPC installation is shown below.

Figure 1.2 A sample FPC installation, (Source: HubPages 2010)

2.2.2 Evacuated Tube Collectors

The collection component of these systems consists of a heat pipe within an evacuated tube as seen below. The heat pipe receives a selective coating similar to the absorber plate in the FPC to maximize the absorption of radiation whilst the vacuum surrounding the tube serves to reduce convective and conductive losses. This allows the ETC to achieve higher operating temperatures than a common FPC. Achievable temperatures range from 50-200˚C (Kalogiru 2009).

Within the heat pipe is a smaller fin/tube, typically copper that contains a liquid-vapour phase change material such as methanol. As it is heated, the methanol begins to vaporize. The vapor rises and travels to the heat sink at the collector header. Here the system HTF flows over the tip/bulb and in doing so is heated. The vapour condenses and flows back into the system and the process repeats.

A typical ETC system schematic is shown below.

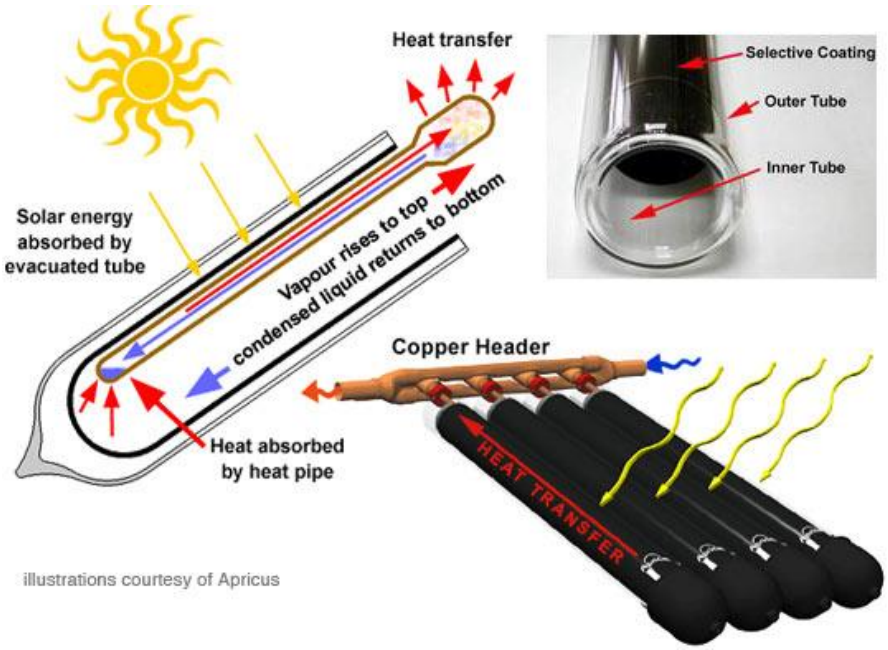

Figure 2.3 The system diagram of an evacuated tube collector, (Source: GreenSpec 2010)

According to Quanshing (2005, pp. 92-93) the ingress of hydrogen atoms into the vacuum is unavoidable due to their size and they destroy the vacuum with time. In order to combat this phenomenon there is a variation on the design known as Dewar tubes. They consist of two concentric glass tubes within one another, the space between which is evacuated. In this way there is no need to penetrate the design to remove heat thus eliminating losses.

ETC have similar orientation requirements to the FPC system though angles cannot so low as to limit the ability of the vapour to rise effectively. They are comparatively expensive as compared to FPC but this is relative to their capabilities.

A variation of this system is as mentioned previously, to array reflective surfaces so that they increase incident radiation on the collector. This essentially produces a variation of the CPC (discussed in next section). Below is a sample ETC installation.

Figure 2.4 A sample ETC installation, (Source: Solar and wind energy, 2010)

Concentrating, Solar Tracking Collectors

It is well known that solar radiation concentrated on a small area leads to a local increase in energy density and heat; one may use the analogy of the child burning ants with a magnifying glass. The same concept applies to the following collectors; by reducing the area on which the solar radiation is absorbed temperatures far higher than those of non-concentrating systems are achievable. These systems exhibit higher thermal efficiency due to the size of the absorption area relative to the collection area. However there are inherent disadvantages to these systems i.e. surfaces must be kept clean or else reflection is inhibited. Also, some mechanism is required to continuously reposition the system to follow the suns path. Concentrating collectors can only utilise the direct beam radiation component of the available radiation.

2.2.3 Compound Parabolic Collector

A typical CPC is shown below

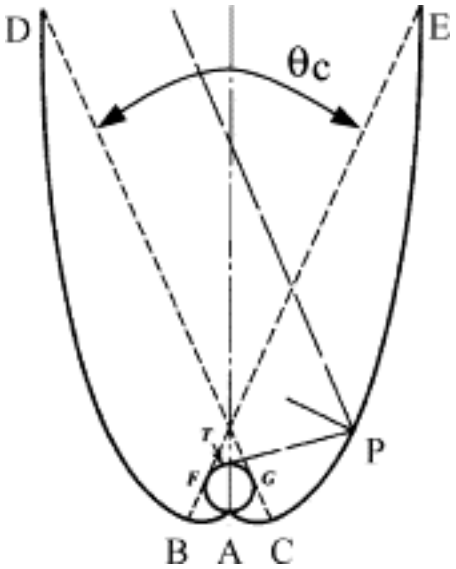

Figure 2.5 A single absorber CPC, (Source: Kalogiru, 2004)

Due to their parabolic nature, CPC can reflect incident radiation from a large range of angles to the absorbing tube (i.e. ETC tube) positioned at the bottom of the collector. They are commonly configured as a trough type arrangement. Often there is a glass cover over them to prevent settling of dust etc that would reduce reflective capability whilst still allowing radiation to pass. They may be arranged as a single absorber system as shown above or with a series of collectors within. They collect only incident radiation that is within the angle θ_c. Consequently, to increase the time over which the collector functions one can simply increase the angle or install a tracking system. They only need to be re-positioned a few times daily.

2.2.4 Parabolic Trough Collector (PTC)

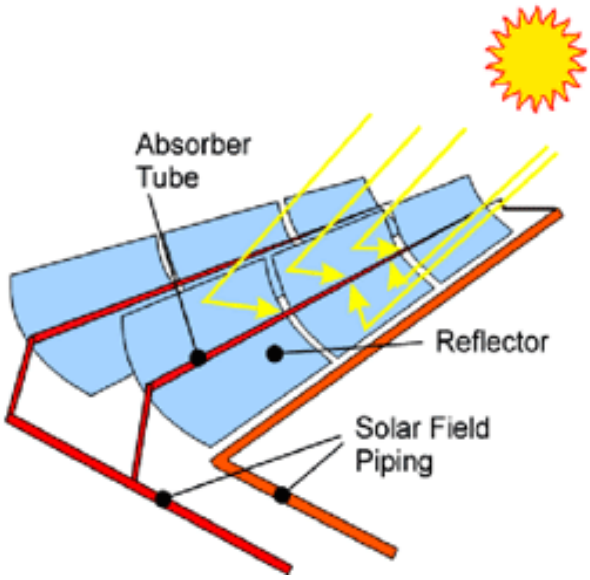

Figure 2.6 Simplified parabolic trough collector, (Source: National Renewable Energy Laboratory, 2010)

PTC's, as the image shows are made of reflective material that focus radiation back to a central collection point. Here, the sun is concentrated by a factor of 80 or more (Quanshing 2005, p.23). These collectors can only focus beam radiation. The receiver is linear and placed along the troughs focus. Within the receiver flows the selected HTF which gains heat as it flows through the system. Receivers are typically metallic with a selective coating to reduce the emittance of thermal energy whilst encouraging high energy absorption. In order to further reduce energy loss from the receiver a glass envelope may be added as it will inhibit convection. Taking this concept a step further the space between receiver and the glass may also be evacuated. However the addition of a glass cover means that reflected radiation must pass through the glass cover to reach the collector. Hence a transmittance loss of about 0.9 is induced when glass is clean (Kalogiru, 2009, p.140). Consequently glass covers will often receive an anti-reflective surface treatment to improve transmissivity. These collectors are capable of temperatures ranging from 50° - 400° through the use of a pressurized collector loop. Consequently they are very suitable

for process heating applications. They are very suitable for process heating applications. The PTC typically utilizes single axis tracking; e.g. oriented N-S longitudinally tracking sun E-W and vice versa. These tracking methods are discussed in detail later on.

Due to their ability to produce high temperature in HTF's these systems are widely used in electricity generation. Power plants that have successfully utilised this approach include America's SEGS (Solar Electricity Generating Systems) plant, a series of smaller capacity fields providing a total capacity of 350MW Kalogiru (2009). Other systems of note are the 64MW "Nevada Solar One" and Spain's 50MW "Andasol 1" and "Andasol 2".

Figure 2.7 A sample PTC installation, (Source: NEP Solar)

2.2.5 Linear Fresnel Collector (LFC)

Linear Fresnel collectors are a similar concept to that of the PTC. They rely on strip mirrors aligned parallel to a fixed receiver, the focal point for their concentrated solar energy. Receiver design is much the same as that of a PTC. The LFC can be visualized as a parabolic trough that has been broken down to individual reflectors. Their greatest advantage is the cost saving as compared to PTC's as flat reflectors are

much cheaper. Also due to their low stance structural requirements are reduced. Similar to PTC they are capable of high temperatures but suffer more from shading/blocking by adjacent units. This can be reduced by increasing the height of the focal point but at the same time this leads to increased cost. Like the PTC they are used primarily in power generation and have much the same requirements for solar tracking.

Figure 2.8 Typical Linear Fresnel Collectors

An extension of this concept is the Heliostat/Power tower arrangement (seen on the next page). Primarily used for power generation and likely beyond the scope of collection for water heating this is merely included for interest

Hundreds of two-axis reflectors surround a tower, their central focus point being the heat collector on the top of the tower. They are used for power generation. Heat in the receiver is transferred to a HTF that runs a closed loop between heat storage and power conversion.

Kalogiru (2004) states this collection system has the following advantages

1. They collect solar energy optically and transfer it to a single receiver, thus minimizing thermal-energy transport requirements;
2. They typically achieve concentration ratios of 300–1500 and so are highly efficient both in collecting energy and in converting it to electricity;
3. They can conveniently store thermal energy;
4. They are quite large (generally more than 10 MW) and thus benefit from economies of scale.

With an array such as this the average solar flux impinging on the receiver has values between 200 and 1000 kW/m2. This high flux allows working at relatively high temperatures of more than 1500 °C and to integrate thermal energy in more efficient cycles

Figure 2.9 "Power Tower" and arrayed heliostats

2.2.6 Parabolic Dish Reflectors (PDR)

Parabolic Dish Reflectors use two-axis tracking to follow the suns motion. The point focus collector in the centre absorbs huge amounts of solar energy and imparts it to a receiver, typically a Stirling engine. The engine generates mechanical energy for use in power generation. PDR's are capable of heating working fluids up to 1500°C. They are capable of >20% efficiency and can also be driven by combustion heat from conventional means should sunlight be insufficient (Quanshing, 2005, p. 25)

According to De Laquil et al., 1993 cited in Kalogiru (2009, p.147) parabolic dishes have several important advantages (over other collection systems):

1. Because they are always pointing the sun, they are the most efficient of all collector systems;
2. They typically have concentration ratio in the range of 600–2000, and thus are highly efficient at thermal-energy absorption and power conversion systems; and
3. They have modular collector and receiver units that can either function independently or as part of a larger system of dishes.

Similar to the Heliostat system mentioned in the previous section this is likely beyond use in a water heating arrangement and is merely included for the fact that it is a widely used solar energy collection device

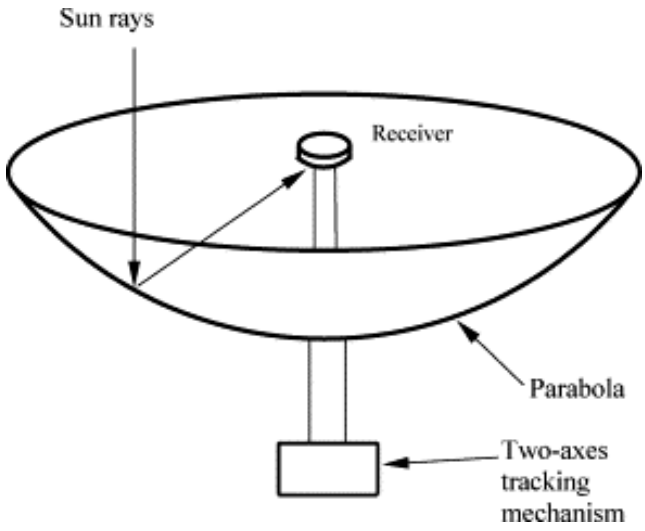

Figure 2.10 A simplified Parabolic Dish Receiver, (Source: Kalogiru, 2004)

2.3 Collector Comparison

The following table is used to summarise the critical information presented above.

Table 2.1 Comparison of collector capabilities

Tracking	Collector Type	Absorber Type	Concentration Ratio	Temp. Range ˚C
Stationary	Flat Plate	Flat	1	30 - 80
	Evacuated Tube	Flat	1	50 -200
	Compound Parabolic	Tubular	1 - 5 ; 5 - 15	60 -240 ; 60 - 300
Single Axis	Linear Fresnel	Tubular	10 - 40	60 - 250
	Parabolic Trough	Tubular	10 - 85	60 - 400
Dual Axis	Parabolic Dish	Point	600 - 2000	100 - 1500
	Heliostat/Central Receiver	Point	300 - 1500	150 - 2000

NOTICE: Sections 2.4 – 2.9 present fundamental solar concepts. Whilst predominantly citing Kalogiru (2009) as it was the most recent and clearly presented, the following information is also presented in;

- **Geyer and Steine (2001);**
- **Kreider, Kreith and Goswami (2000);**
- **Beckman and Duffie (2006); and**
- **Hoogendoorn, Kreider and Kreith (1989)**

2.4 Reckoning of Time

Solar energy calculations use apparent solar time (AST) to express the time of day. AST is based on the angular motion of the sun across the sky and so does not coincide with local standard time (LST). For example, solar noon is the point at which the sun is directly above the observer and occurs at 12:00 AST. However the LST coinciding with this time may be 11:37; LST may be ahead or behind of AST depending on the time of year. Before any calculations can be completed the apparent solar time must be found.

AST can be calculated using the following equation. Its components will be described further.

$$AST = LST + ET \pm 4(SL - LL) - DS \tag{2.1}$$

Where: LST =Local Standard Time
ET = Equation Time [min];
SL = Standard Longitude [degrees];

LL = Local Longitude [degrees]; and

DS = Daylight Savings (0 or 60) [min].

2.4.1 Equation Time (ET)

AST is known to vary from a clock kept running at a uniform rate. This is due in part to minor changes in the earth's orbital velocity at different times of the year. This variation is described primarily by the ET. The equation of time is necessary because the average time for the earth to complete a rotation about its polar axis is not uniform, though the yearly average is 24 hours.

Also, as the earth's orbit is slightly elliptical the earth is further from the sun in June than it is in January. Consequently the speed of orbit is slower than the average from about April to September and faster for October though to March.

Equation Time is represented as:

$$ET = 9.87\sin(2B) - 7.53\cos(B) - 1.5\sin(B)\ \ [minutes] \tag{2.2}$$

Where:

$$B = (N - 81)\frac{360}{364} \tag{2.3}$$

N = day number of the year. For example on February 7, N = 38

2.4.2 Longitude Correction

This is necessary as the local standard time is referenced to the standard meridian, also known as the Greenwich and is located at 0° longitude. As the sun takes 4 minutes to travel 1° of longitude the correction term of *4(SL-LL)* is required.

If the location of interest is east of the standard meridian the longitude correction is added to the clock time i.e. negative sign in front; if west, subtracted.

2.5 Solar Angles; Finding the Sun

It is general knowledge that the earth makes one rotation about the sun in approximately 365.25 days and completes one revolution on its own axis every 24 hours. As observed from earth the sun moves daily across the sky reaching its highest point at noon. With seasonal change from winter to summer, sunrise and sunset points gradually move northward along the horizon and the total number of daylight hours increases. The following subsections detail the fundamental values used to describe the suns position at any given time.

Kalogiru (2009, p.54) states that for simplicity of analysis in solar engineering we utilize the Ptolemaic view of the suns motion i.e. the sun moves about the earth. In this manner its motion is restricted to 2 degrees of freedom, described fully to a stationary observer by 2 angles; α solar altitude and z solar azimuth. These values are not fundamental angles, that is to say they are dependent on specific values of latitude, declination and hour angles. The following subsections provide a brief description of important variables in determining the suns position.

2.5.1 Declination, δ

The earth's axis of rotation is at a constant tilt of 23.45˚ from the elliptic axis, which itself is normal to the plane of the earth's orbital path about the sun. As the earth rotates about the sun it is as if the polar axis is moving with respect to the sun. The angle between the earth-sun line (centre to centre) and the plane of the earth's equator is known as the declination angle. This can also be stated as the angle between the equator and the sun's rays. Kreider, Krieth and Goswami, (2000, p. 24) state that declinations north of the equator are designated as positive. Angles vary from -23.45˚ (summer solstice in southern hemisphere) to 23.45˚ (winter solstice in southern hemisphere). Declination angle passes through zero at the spring and autumn equinoxes as shown in the image below.

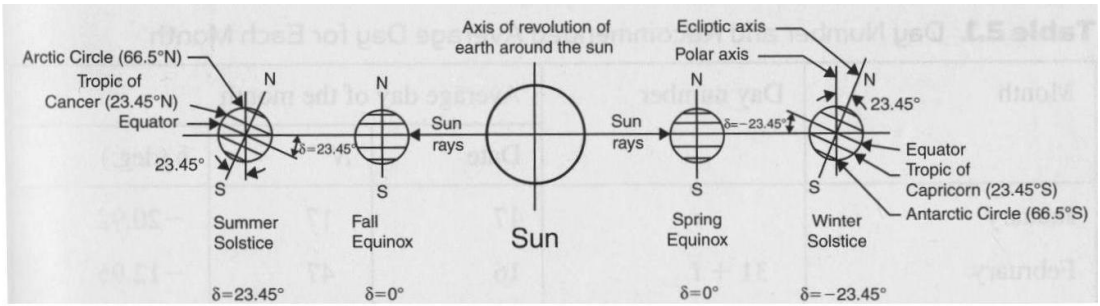

Figure 2.11 Declination of the Sun, (Source: Kalogiru, 2009, p. 55)

The solar declination angle may be estimated using the following:

$$\delta = 23.45 \sin\left[\frac{360}{365}(284 + N)\right] \tag{2.4}$$

Where: N = day number.

2.5.2 Hour Angle, *h*

The hour angle is defined as the angle through which the earth would turn to bring the meridian of the point directly under the sun. It is based on the average time of 24 hours required for the sun to move 360° around the earth (remembering that the Ptolemaic model is in practice). This reduces to 15° per hour.

The hour angle can be expressed by either of the following equations

$$h = \pm 0.25\ (Number\ of\ minutes\ remaining\ until\ solar\ noon) \tag{2.5a}$$

or

$$h = (AST - 12)15 \tag{2.5b}$$

Where: AST = Apparent solar time.

The figure below shows provides a visual representation of the hour, declination and latitude angles.

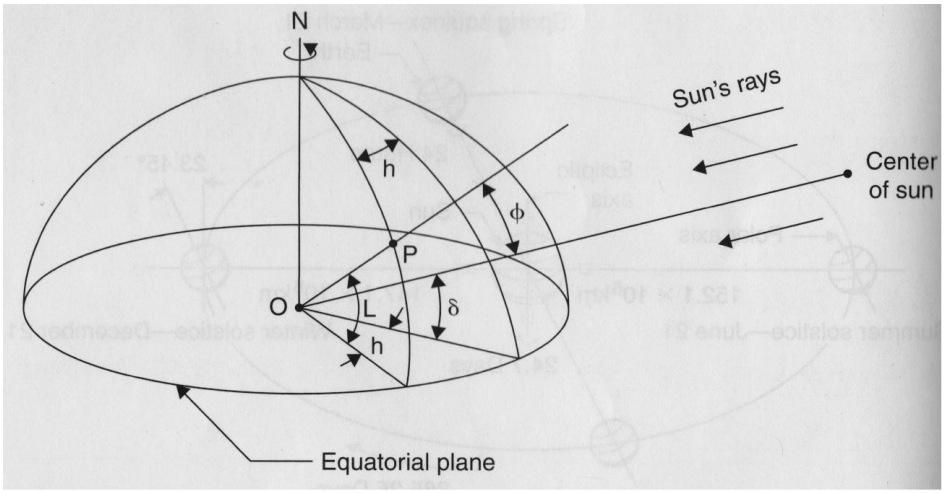

Figure 2.12 Definition of hour, declination and latitude angles, (Source: Kalogiru, 2009, p. 54)

2.5.3 Solar Altitude Angle, α

The solar altitude angle is the angle between the horizontal plane and the suns incident rays. It is related to the solar zenith angle, φ; the angle between incident rays and the vertical. (Kreider, Krieth and Goswami, 2000, p. 24)

It is expressed as follows;

$$\sin(\alpha) = \cos(\varphi) = \sin(L)\cos(\delta) + \cos(L)\cos(\delta)\cos(h) \tag{2.6a}$$

$$\varphi + \alpha = \frac{\pi}{2} = 90° \tag{2.6b}$$

Where: L = local latitude; values north of the equator designated as positive;
φ = solar azimuth angle [degrees];
h = hour angle [degrees]; and
δ = declination angle [degrees].

Note that at sunrise and sunset the solar altitude angle will be 0°. Through rearrangement of equation 2.6a the sunrise and sunset hour angles can be found. These in turn can be used to find sunrise and sunset time in hours from solar noon as well as the length of the day using the equations below. Note that h_{ss} *is* designated as positive in the afternoon.

$$\cos(h_{ss}) = -\tan(L)\tan(\delta) \tag{2.7}$$

Where: h_{ss} = is the hour angle at sunrise and sunset [degrees]

L = local latitude; values north of the equator designated as positive;

h = hour angle [degrees]; and

δ = declination angle [degrees].

As the hour angle is 0° at solar noon, we can find sunrise and sunset time in hours measured from either side as;

$$H_{ss} = -H_{sr} = \frac{1}{15}\cos^{-1}[\tan(L)\tan(\delta)] \tag{2.8}$$

Where: H_{ss} = is the number of hours from solar noon [hours];

L = local latitude; with values north of the equator designated as positive; and

δ = declination angle [degrees].

And the day length in hours as;

$$Day\ length = \frac{2}{15}\cos^{-1}[\tan(L)\tan(\delta)] \tag{2.9}$$

Where: L = local latitude; values north of the equator designated as positive;

δ = declination angle [degrees].

2.5.4 Solar Azimuth Angle, *z*

The solar azimuth angle is the angle formed between the sun's rays measured on the horizontal plane with respect to due North (in Southern Hemisphere) with westward angles designated as positive. Solar noon occurs when the azimuth is exactly 0°.

Solar azimuth, *z* is expressed as;

$$\sin(z) = \frac{\cos(\delta)\sin(h)}{\sin(\alpha)} \tag{2.10}$$

Where: δ = declination angle [degrees];
h = hour angle [degrees]; and
α = solar altitude angle [degrees].

The image below provides a visual representation of the angles presented so far. Note that in this image different terminology is used and corrections are stated below.

- Solar azimuth, *z* is represented below as *A*
- Solar zenith angle, φ is represented as θ. Theta represents the incidence angle which will be discussed in the next subsection. However for a horizontal plane incidence angle and zenith angle are on and the same

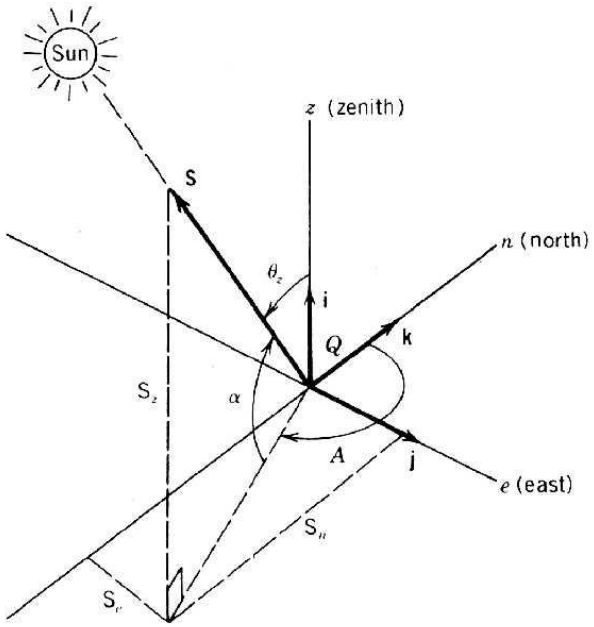

Figure 2.13 Sun/Surface coordinate system, (Source: Geyer and Stine, 2001)

2.5.5 Solar Incidence Angle, θ

This the angle formed between the sun's rays and the normal axis of a surface. As stated previously for a horizontal plane the zenith and incidence angles are the same. The solar incidence angle is used to determine the reduction in incident radiation on the solar collector due to off-normal orientations.

With reference to the image below, Kalogiru (2009, p.61) provides the following general expression for incidence angle on a surface of any orientation.

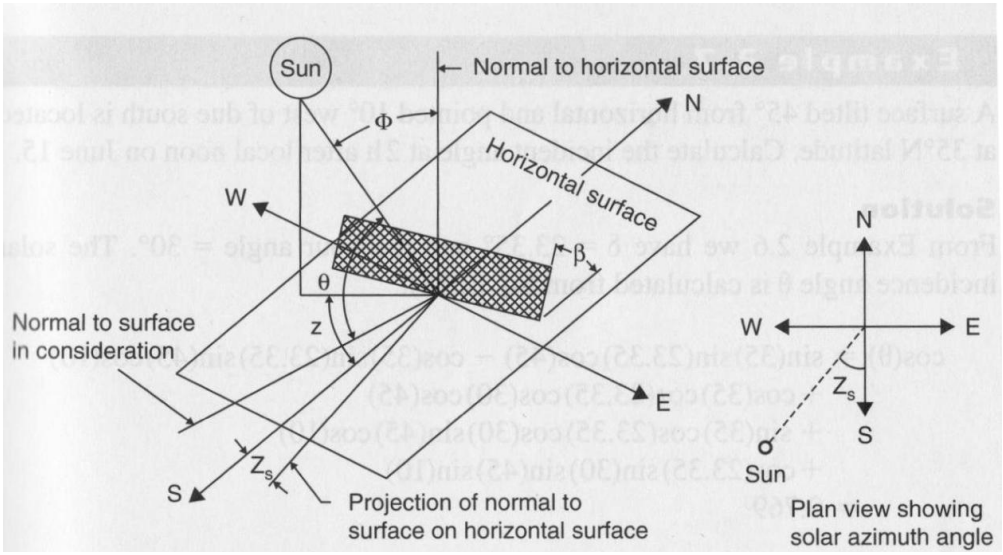

Figure 2.14 Solar Angles, (Source: Kalogiru, 2009, p.61)

$$\cos(\theta) = \sin(L)\sin(\delta)\cos(\beta) - \cos(L)\sin(\delta)\sin(\beta)\cos(Z_s)$$
$$+ \cos(L)\cos(\delta)\cos(h)\cos(\beta)$$
$$+ \sin(L)\cos(\delta)\cos(h)\sin(\beta)\cos(Z_s)$$
$$+ \cos(\delta)\sin(h)\sin(\beta)\sin(Z_s) \quad (2.11)$$

Where: L = local latitude; with values north of the equator designated as positive; and

δ = declination angle [degrees];

β = angle of surface tilt [degrees];

Z_s = surface azimuth angle; the angle between normal to surface measured from due south. Westward values are designated as positive [degrees]; and

h = hour angle [degrees].

However equation 2.11 simplifies dramatically for many cases. For example:

- Horizontal collector – $\beta = 0°$, $\theta = \varphi$
- Vertical collector- $\beta = 90°$, equation 2.11 becomes:

$$\cos(\theta) = -\cos(L)\sin(\delta)\cos(Z_s) + \sin(L)\cos(\delta)\cos(h)\cos(Z_s) + \cos(\delta)\sin(h)\sin(Z_s) \quad (2.12)$$

Incidence angle becomes an important issue when solar tracking is used. Solar tracking and the respective versions of equation 2.11 are presented in the next section.

2.6 Solar Tracking; increasing collection efficiency

Solar tracking collectors are those whose position is constantly readjusted in order to allow them to better follow the sun throughout the day, thus increasing their ability to collect the incident radiation.

Tracking systems are classified based on their axis of rotation; single axis or dual axis (Sorenson, 2000, pp. 382-387). The different tracking modes are listed below.

- Dual axis (fully tracked);
- Polar Axis – tracking EW;
- Horizontal EW axis - tracking NS; and
- Horizontal NS axis – tracking EW.

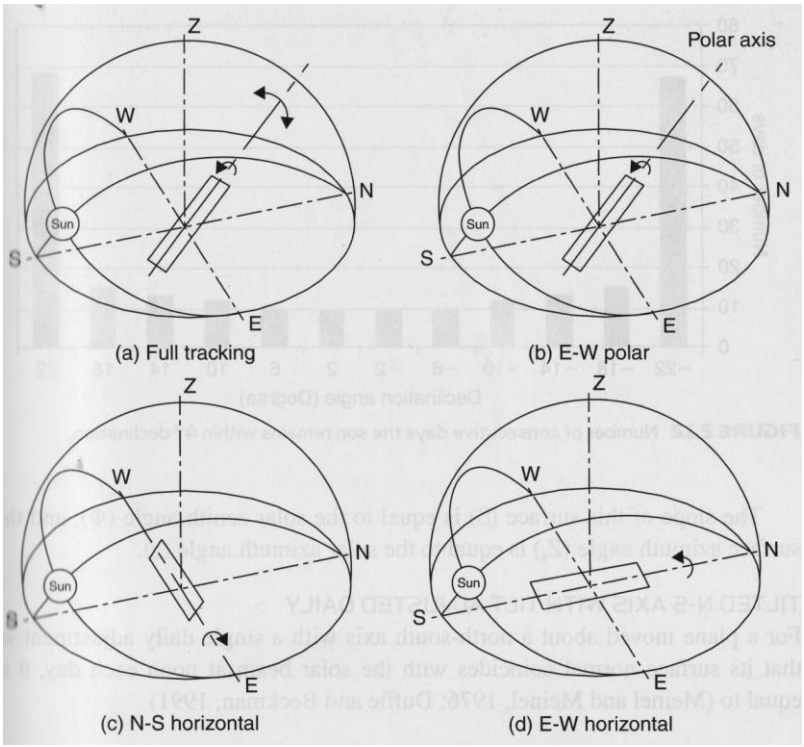

Figure 2.15 The different modes of solar tracking, (Source: Kalogiru, 2009, p.63)

The advantage of a tracked collector is that the incidence angle is kept to a minimum, increasing the incident radiation. This concept will be discussed further at a later time. Consequently each tracking mode has its own equation for incidence angle, i.e. a modified version of equation 2.11.

2.6.1 Dual axis, full tracking

The greatest advantage of a two axis tracking system is that it allows the collection device to follow the suns path exactly by adjusting altitude and azimuth (Quanshing, 2005, pp.45-67).

By keeping the collection surface normal to the solar radiation a full tracking system maintains a constant angle of incidence, θ. (assuming the system operates with complete accuracy)

$$\cos(\theta) = 1 \tag{2.13}$$

i.e. $\theta = 0°$. Consequently this allows the system to collector to receive all of the radiation at the normal to its plane. The collector slope, β is equal to solar zenith angle, φ whilst the surface azimuth angle is equal to the solar azimuth angle *z*.

2.6.2 Polar axis – tracking EW

For a collector rotated about a north south axis at an angle of tilt equal to that of the earth and continuously adjusted to follow the sun will have an incidence angle given by the following equation.

$$\cos(\theta) = \cos(\delta) \tag{2.14}$$

Where: δ = declination angle [degrees].

Consequently during the equinoxes, when δ = 0° the sun will be normal to the collector with maximum cosine effect at the solstices (δ = ±23.45°).Polar axis tracking requires the collector axis, about which rotation occurs to be oriented at an angle equal to that of the local latitude.

The slope of the surface, β as it rotates varies continuously and is described below.

$$\tan(\beta) = \frac{\tan(L)}{\cos(Z_s)}$$

(2.15)

Where: L = local latitude; values north of the equator designated as positive;
Z_s = surface azimuth angle; [degrees]

Due to their upright stance these collectors can suffer from significant shading losses when placed in a multi row array.

2.6.3 Horizontal EW axis – tracking NS

The incidence angle for a collector continuously tracking the sun about a horizontal EW axis is given by Kreider and Kreith, (1978); Beckman and Duffie, (1991) cited in Kalogiru (2009, p.66) to be;

$$\cos(\theta) = \sqrt{1 - \cos^2(\delta)\sin^2(h)}$$

(2.16)

Where: δ = declination angle [degrees]; and
h = hour angle [degrees].

This form of tracking experiences minimal shading. During the summer months it can almost approximate the effect of full tracking but suffers seriously from cosine loss in the winter months. In short the winter performance is much less than summer.

Again the collector slope must change continually and the value required is given by:

$$\tan(\beta) = \tan(\varphi)\,|\cos(z)|$$

(2.17)

Where: φ = solar zenith angle [degrees]; and
z = solar azimuth angle [degrees].

2.6.4 Horizontal NS axis – tracking EW

The incidence angle for a collector continuously tracking the sun about a horizontal NS axis is given by Kreider and Kreith, (1978); Beckman and Duffie, (1991) cited in Kalogiru (2009, p.66) to be;

$$\cos(\theta) = \sqrt{\sin^2(\alpha) - \cos^2(\delta)\sin^2(h)}$$

(2.18)

Where: α = solar altitude angle [degrees];
δ = declination angle [degrees]; and
h = hour angle [degrees].

Due to its orientation this tracking mode gives very little shading loss when arranged in multi row arrays. That is to say that shading is only a problem either very early or very late in the day.

The slope angle required to maintain the tracking is given by:

$$\tan(\beta) = \tan(\varphi)\,|\cos(Z_s - z)| \tag{2.19}$$

Where: φ = solar zenith angle [degrees];

z = solar azimuth angle [degrees]; and

Z_s is determined according to:

$$z > 0°, \qquad Z_s = 90°$$

$$z < 0°, \qquad Z_s = -90°$$

2.6.5 Tracking mode comparison

Due to its reliance on incidence angle the tracking mode selected affects the amount of incident radiation on the collector. The following table provides a comparison of the tracking modes discussed above.

Table 2.2 Solar energy collectors (Source: Kalogiru, 2009, p. 69)

Tracking	Solar energy received kWh/m^2			% to full tracking		
	Equinox	SSolstice	WSolstice	Equinox	SSolstice	WSolstice
Full	8.43	10.6	5.7	100	100	100
N-S Polar Axis; E-W rotation	8.43	9.73	5.23	100	91.7	91.7
E-W Horizontal Axis; N-S rotation	7.51	10.36	4.47	89.1	97.7	60.9
N-S Horizontal Axis; E-W rotation	6.22	7.85	4.91	73.8	74	86.2

Over the course of a year a horizontal N-S trough will collect slightly more energy than its E-W counterpart. It will collect more energy in summer than E-W but less in winter so the choice for orientation depends primarily on the application (Kalogiru, 2004).

2.7 Shadowing effects

When developing a solar energy system one should consider the potential effects of shading. Perhaps the collectors are to be placed close to existing structures to space constraints. As the shadows will drastically affect collector performance it is essential then to be able to predict the amount of shading on a collector be it from a building or simply from adjacent collectors.

Since solar radiation travels a straight path, the shadow projected by a structure is given simply as the following geometric relationship known as the *solar profile angle, p*

$$\tan(p) = \frac{\tan(\alpha)}{\cos(z - Z_s)}$$

(2.20)

Where: α = solar altitude angle [degrees];

z = solar azimuth angle [degrees]; and

Z_s = surface azimuth angle [degrees].

The image below depicts the orientation of values used in determining the solar profile angle.

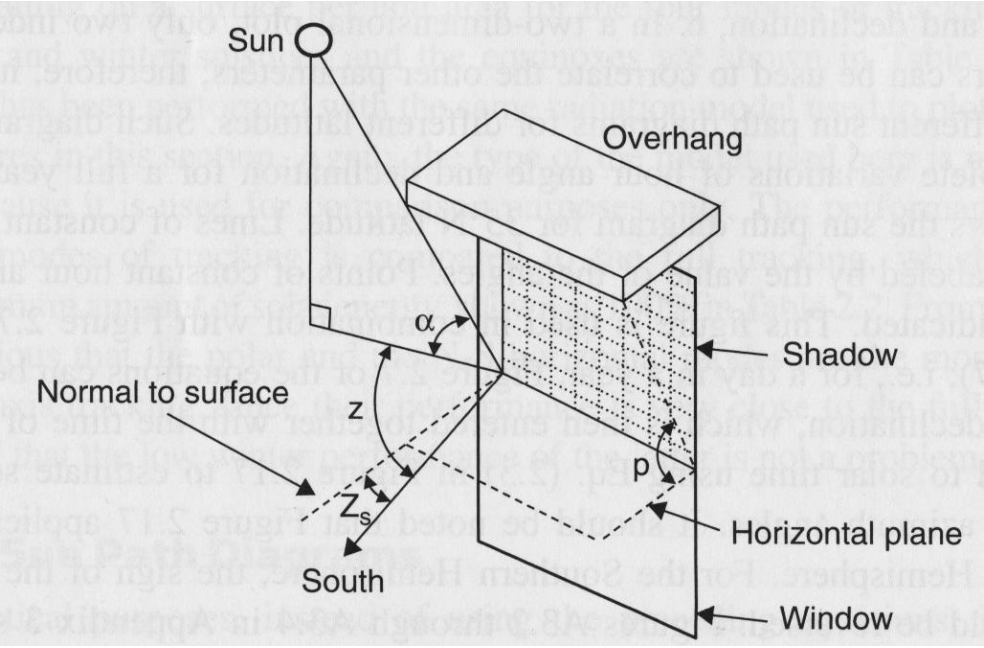

Figure 2.16 The geometric relationship describing solar profile angle, *p*. (Source: Kalogiru, 2009, p. 70)

2.8 Solar radiation

In order to analyse a solar thermal system one must have reliable data relating to the incident solar radiation, commonly termed *insolation*. Insolation is measured as irradiance or energy per unit time per unit area i.e. W/m^2.

Solar energy is electromagnetic radiation with wavelengths from 0.3 μm - >3 μm, (Kreider, Kreith and Goswami (2000, p.38). This range covers ultraviolet, visible and infra-red radiation. However the energy is most dense between UV and infra-red.

As extraterrestrial radiation approaches the earth it must pass through the atmosphere. As it passes begins to enter, part of the radiation is reflected back into space. Once the radiation has entered the atmosphere it is further reduced as it is scattered by dust, aerosols or other particles, or absorbed by water vapour.

Radiation that reaches the earth with no direction change is known as *beam radiation, G_Bn.* Radiation scattered by atmospheric conditions is termed *diffuse radiation, G_D.*

The following image demonstrates the concepts presented above.

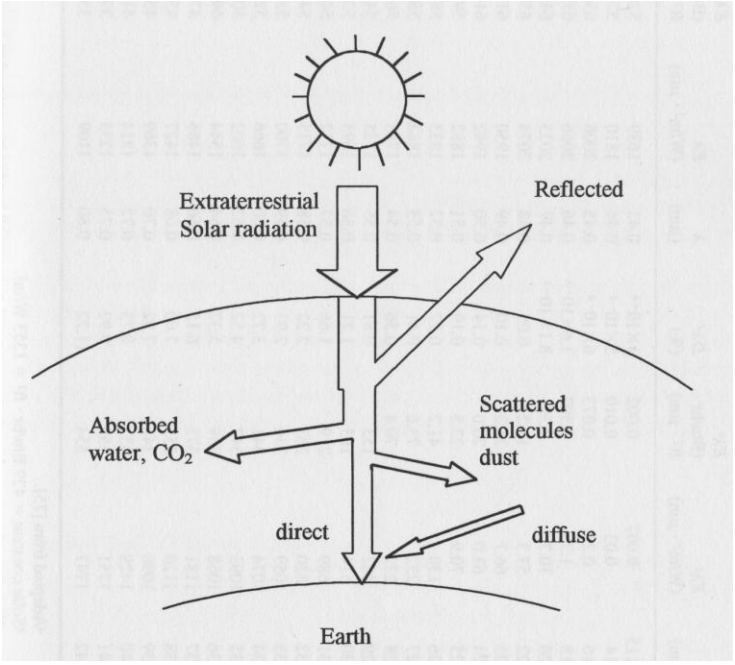

Figure 2.17 Radiation as it passes though the atmosphere, (Source: Kreider, Kreith and Goswami, 2000, p.38)

The best data one can obtain for use in determining insolation on a terrestrial surface is the typical meteorological year (TMY). The TMY provides hourly values for radiation, ambient temperature, wind speed and other such variables that have been averaged over a period of 30 years or more. If a TMY can be obtained for the site of the collectors the analysis is simplified dramatically. However many locations do not have such data. The following paragraphs show a method for estimating the radiation values necessary for collector analysis when a TMY cannot be obtained.

More commonly there is access to long term monthly average daily insolation data for the collector site. One may also obtain daily mean total insolation (beam + diffuse radiation) on a horizontal surface. Such information is commonly available through the Bureau of Meteorology.

Once this basic information is obtained, both Kreith, Kreider and Goswami (2000) and Kalogiru (2009) describe the next step to be the definition of the monthly clearness index, $\overline{K_T}$.

$$\overline{K}_T = \frac{\overline{H}}{\overline{H}_0}$$

(2.21)

Where: $\overline{H}$ = monthly average total insolation on a horizontal terrestrial surface [MJ/m^2-day] (obtained for example from Bureau of Meterorology); and

$\overline{H}_0$ = monthly average daily total insolation on a horizontal extraterrestrial surface [MJ/m^2].

There are methods for calculating $\overline{H}_0$ but the data commonly comes in the form of a table that lists its value for each month as a function of latitude, and a representative day for the month. A small portion of such a table taken from Kalogiru (2009, p.94) is given below for demonstration.

Table 2.3 Monthly average daily extraterrestrial insolation on a horizontal surface, [MJ/m^2]

Latitude	Jan-17	Feb-16	Mar-16
60 S	41.1	31.9	21.2
55 S	41.7	33.7	23.8
50 S	42.4	35.3	26.3
45 S	42.9	36.8	28.6

As previously mentioned, in order to analyse the performance of a solar collector the hourly values of radiation are required. Using the relationship established in (2.21) the Liu and Jordan (1977) and Collares-Pereira and Rable (1979) cited in Kalogiru, (2009) empirical correlations can be used to find the hourly values.

Liu and Jordan correlation

$$r_d = \left(\frac{\pi}{24}\right)\frac{\cos h - \cos h_{ss}}{\sin h_{ss} - \left(\frac{2\pi h_{ss}}{360}\right)\cos h_{ss}} \tag{2.22}$$

Where: r_d = ratio of hourly diffuse radiation to daily diffuse radiation;
h_{ss} = sunset hour angle [degrees]; and
h = hour angle taken at the midpoint of each hour [degrees].

$$\frac{\overline{H}_D}{\overline{H}} = 1.390 - 4.027\overline{K}_T + 5.531\overline{K}_T^2 - 3.108\overline{K}_T^3 \tag{2.23}$$

Where: $\overline{H}_D$ = monthly average daily diffuse radiation on horizontal surface [MJ/m^2-d];
$\overline{H}$ = monthly average total insolation on a horizontal terrestrial surface [MJ/m^2-day] (obtained for example from BOM); and
$\overline{K}_T$ =monthly clearness index as defined in (2.21).

Collares-Pereira & Rable correlation

$$r = \frac{\pi}{24}[a + b\cos(\theta)]\frac{\cos(h) - \cos(h_{ss})}{\sin(h_{ss}) - \left(\frac{2\pi h_{ss}}{360}\right)\cos(h_{ss})} \tag{2.24}$$

Where: r = ratio of hourly total radiation to daily total radiation;
h_{ss} = sunset hour angle [degrees];
h = hour angle taken at the midpoint of each hour [degrees];
$a = 0.409 + 0.5016\sin(h_{ss} - 60)$; and
$b = 0.6609 - 0.4767\sin(h_{ss} - 60)$;

The solving of these equations provides one with the values of $\bar{H}_D$, r and $r_{d.}$

Now,

$$Average\ hourly\ total\ radiation = r \cdot \bar{H}$$

$$Average\ hourly\ diffuse\ radiation = rd \cdot \bar{H}_D$$

The hourly beam radiation is simply hourly total radiation less hourly diffuse radiation.

2.8.1 Radiation on a Tilted Surface

Collectors are often installed not horizontally but at an angle in order to increase the amount of radiation intercepted and to reduce cosine losses (associated with the incidence angle). The same principle applies to surfaces that track the sun. As previously stated, most measured solar radiation data is measured with respect to a horizontal surface.

For a flat, tilted surface, the total radiation absorbed is given by:

$$G_t = G_{Bt} + G_{Dt} + G_{Gt} \tag{2.25}$$

Where : G_{Bt} = beam radiation [W/m^2];
G_{Dt} = diffuse radiation [W/m^2]; and
G_{Gt} = ground reflected radiation [W/m^2].

The beam component is described by:

$$G_{Bt} = G_{Bn}\cos(\theta) \tag{2.26}$$

Where : G_{Bn} = direct beam radiation [W/m^2]; and
θ = incidence angle .

And so we see that the greater the angle of incidence, less radiation the collector can utilise.

The diffuse component is described by:

$$G_{Dt} = \int_0^{\frac{\pi}{2}-\beta} G_R\cos(\varphi)\,d\varphi + \int_0^{\pi/2} G_R\cos(\varphi)\,d\varphi \tag{2.27}$$

Where : G_R = diffuse sky radiance [W/m^2]; and
φ = zenith angle.

The ground reflected component is described by:

$$G_{Gt} = \int_{\frac{\pi}{2}-\beta}^{\frac{\pi}{2}} G_r \cos(\varphi)\, d\varphi \tag{2.28}$$

Where : G_r = isotropic ground reflected radiance (W/m^2); and
φ = zenith angle.

The presented above are common to both Kreith, Kreider and Goswami (2000) and Kalogiru (2009).

2.9 Heat storage

Solar thermal energy is commonly stored in one of two ways; as sensible heat or latent heat. By including a thermal storage component in a solar thermal design there can be better utilisation of collected energy. For example if the field is generating thermal energy at a rate greater than that at which it is being used the excess energy can be stored and called upon later when insolation has dropped. The selection of a storage system depends largely on the application. Without going into too much detail other factors to consider during selection are the location of storage devices and the rate at which they lose heat. The conceptual design produced by this project is anticipated to be an ancillary 'boost" system and as such there is currently no intention to include storage in the system; this will be elaborated on later.

However the following storage methods are discussed briefly to provide greater understanding of solar thermal system design.

2.9.1 Sensible heat

"Sensible heat" is the form of heat storage that is most commonly encountered in day to day life. It is simply achieved through raising the temperature of an object without causing phase change or chemical composition.

The amount of energy stored through increasing the temperature of an object with mass, *m* and specific heat c_p from T_1 to T_2 under constant pressure is given by:

$$Q = m \int_{T_1}^{T_2} c_p \, \Delta T$$

The most common medium for sensible heat storage is water; favored because of its high specific heat. Water can store higher levels of heat if maintained under pressure to inhibit boiling. Other common mediums include oils, rocks, ceramics and salts. (Kreith, Kreider and Goswami, 2000). Two common mediums of interest expanded upon below.

Graphite - Pure graphite has been found to be an effective medium for heat storage. It is not uncommon to have graphite collectors atop power tower systems. Graphite may be heated by absorbed radiation (direct heating) or it may be located elsewhere for storage and heated indirectly by a HTF. The energy is regained at a later time by passing a cooler HTF though the system.

Molten Salts - Molten salts have been found to be very good HTF/storage mediums and are commonly used in power tower collection. They are typically liquid at atmospheric pressure, cheap and efficient. Most commonly used is salt peter (60% Sodium Nitrate and 40% Potassium Nitrate). Salt peter melts at 220°C and is stored, liquid at 290°C in tanks. Heat can be efficiently stored for up to one week.

2.9.2 Latent heat

Thermal energy may be stored as latent heat in a material that undergoes phase change transformation. Phase change materials are those substances possessing high heat of fusion. Heat of fusion refers to energy that must be absorbed or released to change phase of 1mol of material. Initially, a solid-liquid PCM will act like a sensible heat storage medium. That is the temperature rises accordingly as heat is absorbed. However when the phase change temperature is reached they absorb large amounts of heat whilst remaining at an almost constant temperature until all of the material has changed. The process is fully reversible.

According to Kreith, Kreider and Goswami, (2000, pp. 176-178), if a material with phase change temperature T_m is heated from T_1 to T_2 (where $T_1<T_m<T_2$), the thermal energy, Q stored in the mass, m is equal to:

$$Q = \int_{T_1}^{T_m} mc_p\,\Delta T + m\lambda + \int_{T_m}^{T_2} mc_p\,\Delta T$$

Where: λ = heat of phase transformation.

Geyer and Stine present the following example. The PCM of interest is Sodium Hydroxide (NaOH). NaOH has a latent heat of fusion of 156 kJ/kg. That is to say that as I kg of NaOH melts it has absorbed 156 kJ of thermal energy. This is in contrast to heat transfer oil with a latent heat of fusion 2.1 kJ/kg-K. In order to absorb the same amount of energy the oil would need to increase in temperature but 74 ºC.

There are four kinds of phase transformation.

- Solid ⇔ Solid
- Solid ⇔ Vapour

- Liquid ⇔ Vapour
- Solid ⇔ Liquid

Solid-Liquid is most common in solar applications. There are typically two classes of PCM; organic and inorganic. Organic PCM's include Paraffin (C_nH_{2n+2}) and Fatty acids ($CH_3(CH_2)_{2n}COOH$). Inorganic PCM's are typically salt hydrates.

2.9.3 Thermochemical energy storage

This method of energy storage is thermochemical energy storage. It is however at this stage still very much theoretical and there is no solar thermal system known to be running such a method at this stage. Thermochemical energy storage is achieved through the use of thermal energy to reversibly break chemical bonds. Breaking a bond requires a great deal of energy and whilst it remains broken the energy is stored. The product or products of a thermochemical reaction are usually very stable at ambient temperatures. At a later stage, at an increased temperature the process is reversed. The original compound forms and the heat is released. Geyer and Stine (2001) provide the following example.

Consider the thermal dissociation of water. When its temperature exceeds 2000 ºC it begins to separate into its components

$$2H_2O + \text{thermal energy} = 2H_2 + O_2$$

At ambient temperature, hydrogen and oxygen will not react. However in the presence of heat the reaction is explosive.

$$2H_2 + O_2 = 2H_2O + \text{thermal energy}$$

So we see the attractiveness of this heat storage method. High amounts of energy can be stored in a small amount of mass. As components are non-reactive at ambient temperature they can be stored indefinitely (as opposed to latent and sensible systems which require insulation). The research into this area is ongoing.

2.10 Solar thermal water heating

In the early stages of the research, common solar water heating systems were examined. Findings showed a great deal of information on the design of domestic/small scale heating systems. This research was omitted from the final review due to its irrelevance.

Naturally the water heating component of this project will be quite different to solar hot water systems used in the domestic market. However the same basic principles apply. It became clear that on an industrial scale the process of water heating system design is somewhat simpler. Industrial process heat, in this case from a solar collection field, heats a fluid. If the working fluid through the collectors is the heated water required then this is known as direct heating. Alternatively if a HTF is passed through the collector it must then pass through a heat exchanger to heat the water. This is termed indirect heating. Water heating systems may be active (pumped) or passive (fluid moves due to convection).

Often storage for the water once heated must be considered. However as the conceptual system is ancillary any heated water is plumbed directly into the existing infrastructure and so research into heated water storage was not carried out.

2.11 Solar thermal air cooling

Kalogiru (2009) states that solar thermal cooling, especially at an industrial level is typically achieved through the use solar sorption systems. Note that there are other solar related methods to cool air but are not nearly effective enough to be considered as an alternative for the system.

A *sorbent* is a material capable of drawing and holding other gasses or liquids. A *desiccant* is a sorbent that works very well with water. Depending on the way the desiccant behaves as it draws the moisture to itself defines the process as either

adsorption or *absorption*. These processes are reversible. During the adsorption process, the desiccant does not change at all but for the increase in weight due to the particles drawn in; a similar concept to a sponge that has soaked up water. Absorption however changes the desiccant. A well known example of this process is the way table salt will change from a solid to a liquid as it absorbs the moisture around it. Solar thermal air cooling is then achieved in one of two ways, adsorption cooling or absorption cooling. Both systems mimic the operation of the traditional vapour-compression cycle and are explained now in detail.

2.11.1 Adsorption cooling

The amount of adsorbate drawn to an adsorbent depends largely on the mixture between the two and the adsorbate vapour pressure. As adsorbate concentration is dependent on temperature the adsorbent can be manipulated to adsorb or desorb the adsorbate through an increase/reduction of temperature under constant pressure (Kalogiru, 2009). This property is the driving force behind the adsorption refrigeration cycle.

Common working pairs in adsorption cooling systems are silica gel – water, zeolite – water and zeolite – methanol.

A simplified schematic of a typical adsorption machine is shown below.

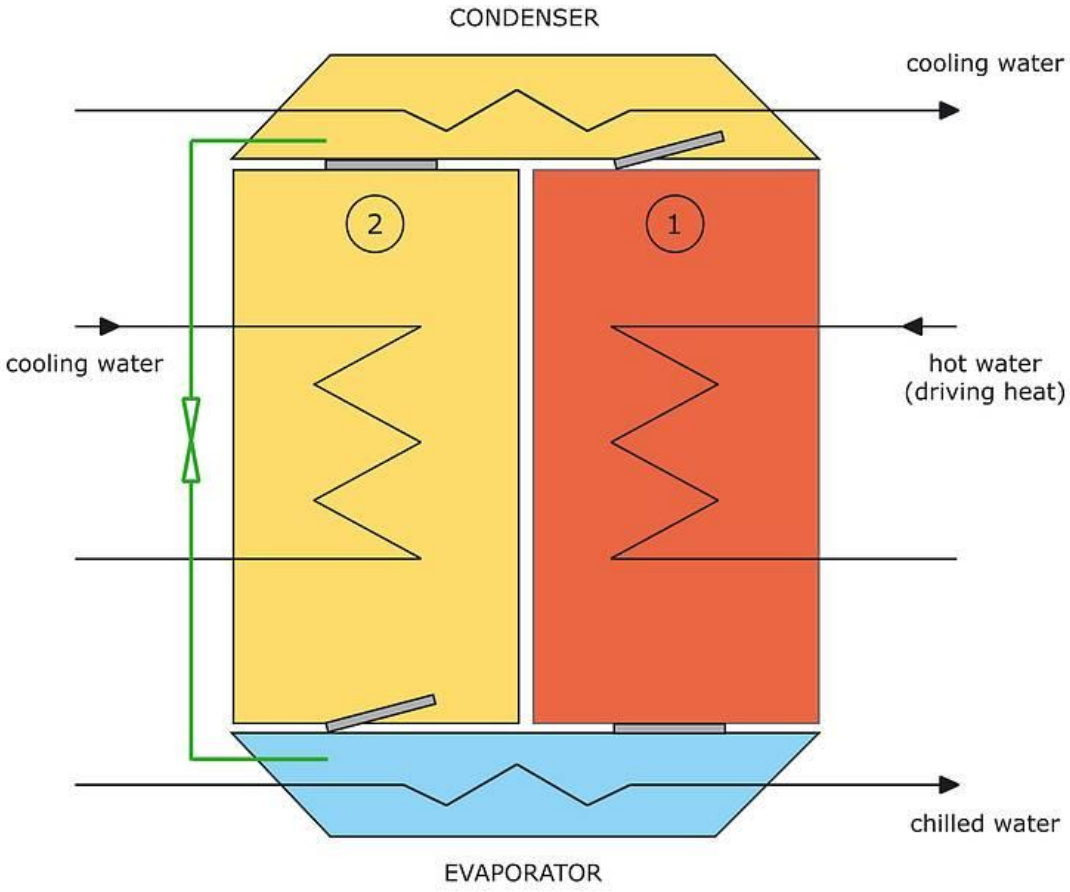

Figure 2.18 A simplified adsorption chiller, (Source: Solair, 2009)

As shown in the image above there are two separate sorbent compartments, one serves as an evaporator and the other a condenser. The sorbent in the primary compartment is continuously regenerated by a heated fluid entering from the collector loop (in this case water). The primary compartment continually desorbs water vapor to the evaporator. The sorbent in the secondary compartment adsorbs water vapor entering from the evaporator. The secondary compartment must be continuously cooled to ensure adsorption is uninterrupted. Chilled water leaves the evaporator to pass through an air-water heat exchanger.

With an input of 80 °C to the primary compartment these systems can achieve a COP of approximately 0.6 (COP is defined as the ratio of the cooling effect to the heat input). Chillers commonly produced are capable of refrigeration output of up to 500 kW.

Due to the limited use of these systems they are relatively expensive to purchase.

2.11.2 Absorption cooling

Absorption refers to the process by which a fluid can attract retain moisture. This is done using substances known as desiccants, materials that absorb moisture. The level of absorbed moisture is dependent on temperature. Absorption cooling takes place via a process that is similar to traditional vapour-compression air conditioning, the primary difference being the way the refrigerant is compressed. As mentioned above, the success of the system depends on the selection of a suitable working fluid pair. Kreider, Kreith and Goswami (2000, p. 270) gives the following ideal properties for a working pair:

- No solid phase absorbent;
- A refrigerant that is more volatile than the absorbent. This ensures that separation will occur easily;
- An absorbent with a strong affinity for the refrigerant under absorption conditions;
- Stability of components to ensure long term functionality;
- The refrigerant should have large latent heat; and
- Low fluid viscosity to reduce power consumed in pumping. This also improves heat transfer.

There are two working pairs that satisfy these parameters. They are Ammonia-Water (NH_3–H_2O) and Lithium Bromide-Water (LiBr–H_2O). The two different refrigerant types have different heating requirements and efficiencies. According to Kalogiru (2004), the NH_3–H_2O system requires generator temperatures in the range of 125–170 °C and delivers a COP of 0.6 - 0.7. The LiBr–H_2O system operates at a higher generator temperature of 70–95 °C has COP between 0.6 and 0.8

Both systems must be supplied with cooling water (typically provided by cooling towers) for use in the absorber and condenser. The information above agrees exactly with (Sorenson, 2000) who also states that LiBr-H_2O systems are well suited to flat plate collectors. LiBr systems are more popular not only due to superior performance but also because it is less toxic than ammonia.

A single stage absorption chiller is presented below.

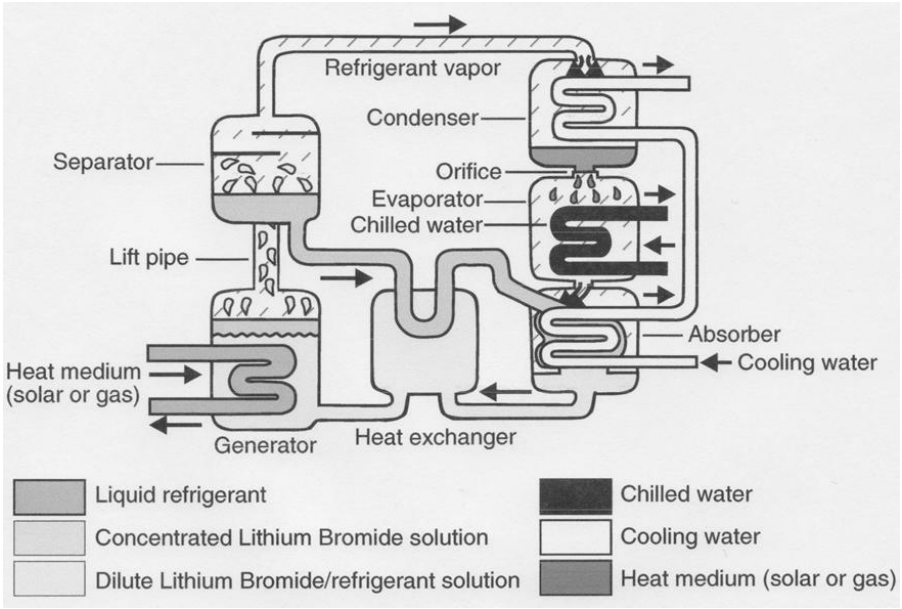

Figure 2.19 A single stage LiBr absorption chiller, (Source: Energy Solutions Centre)

Herold, Klein and Radermacher (1996) summarise the cycle as follows:

- The evaporator generates chilled water at 5 – 10 °C. The chilled water is pumped to an air-water heat exchange and the air distributed accordingly. Water is chilled as the refrigerant water at very low pressure absorbs heat and vaporizes.
- The refrigerant (water) vapor enters the absorber. Here there is a concentrated LiBr solution which as previously stated has an affinity for water vapour. The LiBr solution absorbs the vapour as it flows over the absorber coil.
- Diluted LiBr flows from the absorber to a solution heat exchanger. This essentially serves to increase system efficiency by pre-heating the diluted solution
- Once in the generator the weak solution is exposed to the heat source under low pressure. Consequently the water boils out of the solution and forms a high temperature and pressure refrigerant vapour.
- The vapour rises through the separator to the condenser where it collects on the surface of the cooling water coil. The liquid collects and passes once more into the evaporator to repeat the cycle.

Note that the performance of an absorption chiller can be improved through the addition of a secondary generator. Instead of diluted LiBr flowing directly back from the primary separator to the absorber via the solution heat exchanger it is passed to a secondary generator. The high temperature and pressure refrigerant vapour just generated leaves the separator and flows through a coil in the secondary generator. In this way a second round of refrigerant vapour is produced leading to a dramatic increase in the performance of the entire systems. 2 stage absorption chillers are known to achieve COP of 0.9-1.5. They do require a higher input temperature to accommodate the double generation; generally an input temperature to the primary generator of >145 °C is necessary.

A 2 stage system is shown below.

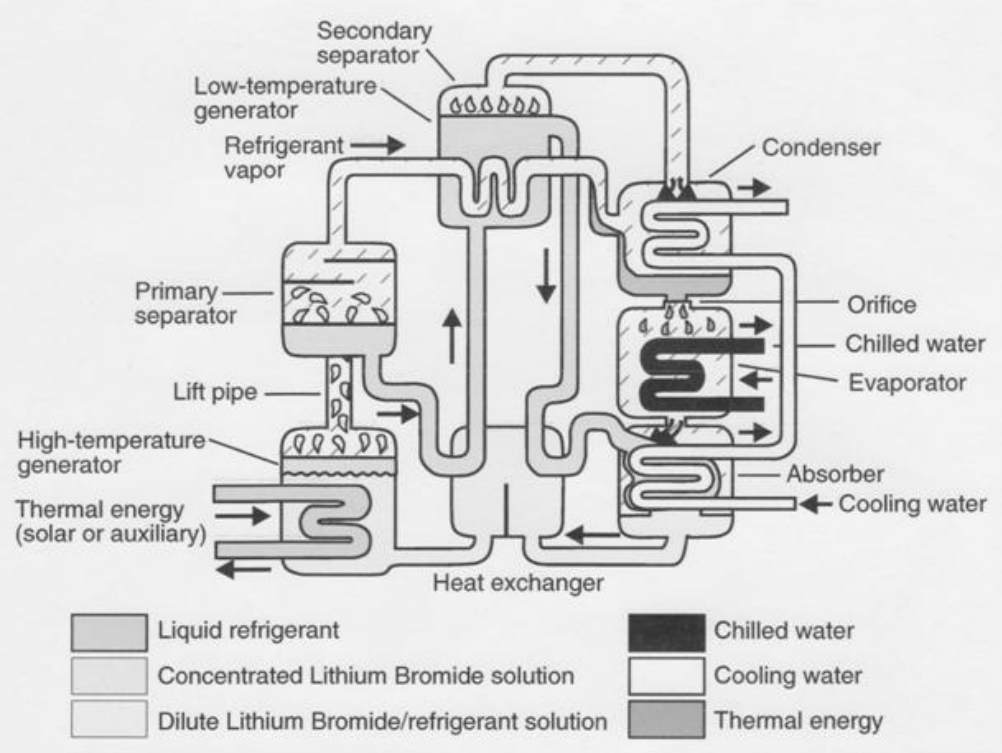

Figure 2.20 A two stage absorption chiller, (Source: Energy Solutions Centre)

2.12 Utilisation of solar thermal energy in the meat processing industry

Initial research suggests that there is little to no utilisation of solar thermal energy for water heating or cooling within the meat processing industry; even though the potential of such systems has been identified previously by (Aye & Fuller, 2007, p. 9) and (Australian Industry Group, n.d)

Sustainable practice in the meat processing industry seems to be focused elsewhere at this time. As far back as the late '90s there has been pressure to reduce water consumption within abattoirs through increasing system efficiency and water treatment/re-use. Meat and Livestock Australia has produced resources for industry such as (Meat and Livestock Australia, 1997) and continues to do so. MINTRAC (National Meat Industry Training Advisory Council Limited) have also been guiding the industry toward efficient water usage beginning with the inclusion of a best practice module in their Diploma of Meat Processing (Meat and Livestock Australia, 1998). The government too provides resources, both factual and monetary (in the form of rebates) to encourage sustainable use (Department of the Environment, Climate Change and Water, 2008)

Recently there has been increased used of co-generation plants within industry, typically powered by natural gas. These systems, whilst expensive to implement are incredibly efficient due to the fact that they provide both electricity and water heating/steam simultaneously. One such case is found at KR Castlemaine Foods in Toowoomba where they significantly reduced greenhouse emissions through cogeneration. The system provides for ALL of the abattoirs electricity needs, even exporting 1.9 MW of power into the local grid; both of the original boilers have been made redundant as all steam and water heating required is provided for by the one unit (DDC Energy Services, 2007). A similar is that of Midfield Meats, Warnambool, VIC. They received a government grant towards the installation of their cogeneration system (Minister for Regional and Rural Development, 2009). Its system, similar to that of KR Castlemaine provides 80% of their power needs and provides steam/water heating with waste heat for an overall system efficiency of approx. 89% (EcoGeneration, 2010).

There is also research underway into the use of biogas for combustion. This biogas is typically on site through the anaerobic digestion/fermentation of organic matter (such as solid wastes from abattoirs). This biogas is made primarily of methane and can be further purified for combustion i.e. cogeneration (Biogas, 2010)

2.13 Conclusions

This literature review serves as the starting point for the conceptual design. It has given an overview of various devices used for energy collection, fundamental solar principles, heat storage methods as well as both water heating and air cooling options. It became apparent that whilst there is a great deal of generic information on energy collection and basic system design available on the internet, the best sources of information when beginning the research project were solar engineering texts as they cover all aspects of design. The following books were relied upon extensively throughout the project and have been invaluable;

- Kalogiru, SA 2009, *Solar Energy Engineering – Processes and Systems*, Elsevier, San Diego.
- Goswami, DY, Kreider, JF & Kreith, F 2000, *Principles of Solar* Engineering, 2nd edition, Taylor & Francis, Philadelphia
- Geyer, M, Stine, WB 2001, *Power From The Sun*, (a free online book at powerfromthesun.net)

It was these texts that bridge the gap between the generic/domestic style information that is typically found on the internet to the comprehensive information needed for design on an industrial scale. It is expected therefore, that this project will bring something novel to body of knowledge in that solar thermal collectors used primarily for electricity generation will be adapted to provide water heating at an industrial level whilst simultaneously providing refrigeration.

It would seem that the meat processing industry is very interested in renewable energy utilisation, at the very least in increasing efficiency to reduce energy/resource consumption. However the focus seems to be more on cogeneration systems as they provide not only electricity but also steam/hot water. Their main drawback though is that they are incredibly expensive to implement. Should this project prove successful in producing a useful solar thermal system it may provide abattoir operators with an opportunity to reduce emissions and overheads for a fraction of the cost.

Chapter 3 – The Design Process

3.1 Introduction

This chapter will firstly outline the design requirements and constraints that apply to the conceptual system. Once the components have been broadly specified, the methods used to analyse the system components are presented; the primary focus being the analysis of the solar thermal collectors. The results of this analysis will provide the information needed to clearly define component requirements.

3.2 The Design Process

The design parameters for the conceptual solar thermal system will dictate its overall design. They are outlined below

The design should:

- Integrate with existing infrastructure at the abattoir. It is to be an ancillary system, a "boost" system rather than a sole energy solution. The collectors are to be roof mounted. Roof space available is approximately 2600 m^2. For simplicity of analysis this is treated an area 50 m x 50 m.
- Be as efficient as possible.
- Provide chilled air.
- Provide heated water.
- Be easy to maintain; Low frequency periodical maintenance is ideal.
- Not require heat storage. Heat storage is typically needed for night time operation and this plant is only run during the day. Although refrigeration

systems still run at night that will remain the concern of the existing systems. Whenever solar energy is available it is used by the system immediately.

3.2.1 Component Selection

After spending considerable time considering the systems potential components it became clear that by nature they will exhibit a dependence on one another. Based on this reasoning it became apparent that the air cooling system would be the defining factor in the selection the other components. This is because the energy collectors will need to provide enough power to drive the chiller effectively. The outputs from the chiller then determine the temperature of fluids that are provided to the heat exchangers and ultimately the temperature of fluid reentering the collector field.

Air cooling

Based on the findings of Chapter 2 there were two alternatives for solar thermal refrigeration; Adsorption and Absorption chillers.

Recall that adsorption systems are typically only capable of COP <1 and utilise lower temperature fluids. The absorption systems typically have a COP in excess of one with the two stage systems capable of up to 1.5.

Based simply on the fact that a two stage absorption system provides greater cooling effect per unit of heat input when compared to both the single stage system and the adsorption method it was chosen to be the air cooling device within the system. The chosen working fluid was Lithium Bromide–Water as it provides the greatest performance. Therefore the energy collection system needed to be able to provide temperatures in excess of 150 °C at the flow rate required by the chiller.

Energy Collection

The energy collection devices are the heart of the system. Their ability to efficiently utilise the incident solar radiation impacts the performance of the chiller system and thus dictates the success of the design.

The various collector types commonly used in solar thermal systems were presented in Chapter 2. There, the findings of this research were summarised in table form and are presented again for convenience below.

Table 3.1 Solar Energy Collectors

Tracking	Collector Type	Absorber Type	Concentration Ratio	Temp. Range ˚C
Stationary	Flat Plate	Flat	1	30 - 80
	Evacuated Tube	Flat	1	50 -200
	Compound Parabolic	Tubular	1 - 5 ; 5 - 15	60 -240 ; 60 - 300
Single Axis	Linear Fresnel	Tubular	10 - 40	60 - 250
	Parabolic Trough	Tubular	10 - 85	60 - 400
Dual Axis	Parabolic Dish	Point	600 - 2000	100 - 1500
	Heliostat/Central Receiver	Point	300 - 1500	150 - 2000

From the information above, the Parabolic Trough Collection system was deemed the best choice for the design. The justification for this choice is as follows:

- The PDR and central receiver systems are ruled out as they are primarily designed for electricity generation.

- The FPC, ETC and CPC systems are not capable of providing the heat input required by an absorption chiller.
- Linear Fresnel systems suffer from higher levels of shading loss due to their low stance and close proximity to one another.
- Parabolic troughs are widely used for the collection of process heat (recall the power stations listed in Chapter 2). Due to their high concentration ratio they are easily capable of providing heated fluid within the range required by 2 stage absorption chillers (earlier stated to be 150 – 220 °C).

A parabolic trough collector requires a single axis tracking system to constantly track the sun if it is to minimize the cosine loss in incident radiation. The table below was also presented in Chapter 2 and provides a comparison of the various tracking methods available.

Table 3.2 Tracking mode comparison

Tracking	Solar energy received kWh/m^2			% to full tracking		
	Equinox	SSolstice	WSolstice	Equinox	SSolstice	WSolstice
Full	8.43	10.6	5.7	100	100	100
N-S Polar Axis; E-W rotation	8.43	9.73	5.23	100	91.7	91.7
E-W Horizontal Axis; N-S rotation	7.51	10.36	4.47	89.1	97.7	60.9
N-S Horizontal Axis; E-W rotation	6.22	7.85	4.91	73.8	74	86.2

The E-W horizontal; N-S tracking system is very efficient during the summer months and has reasonable spring/autumn performance. However its winter performance is very poor. The N-S horizontal; E-W system exhibits a relatively constant level of energy collection. As previously mentioned, this means that the E-W tracking system will collect more energy over the year than its N-S counterpart.

Based on the reasoning presented above a field of parabolic trough collectors tracking the sun as it moves from east to west, tracked about a north-south axis of rotation was selected as the energy collection device for the system.

Heat exchangers

Heat exchangers are the last crucial component in the design of the system. Essentially there will be two heat exchangers required. The first is needed to remove the heat from ambient air using chilled water produced by the absorption chiller. The second is used to heat water from ambient temperature supply to the 84 °C required in the abattoir. The type and size of these heat exchangers is considered once the heat exchange requirements have been clearly specified.

3.2.2 The Initial Design

In summary the system will be comprised of:

- An energy collection field that consists of horizontal parabolic trough collectors that track the suns path E-W about a N-S axis. The approximated area available for the collectors is 2600 m^2.
- A two stage absorption chiller utilizing LiBr-H_2O working fluid; and
- Two heat exchangers to provide chilled air and heated water.

An initial system schematic is given on the next page. The process is described as follows;

- The heat transfer fluid is pumped into the collector field. As it flows through the system the fluid is heated to in excess of 145 °C.
- The fluid leaves the collectors and enters the generator of a 2 stage absorption chiller. It leaves the generator, now at reduced temperature and is passed on to a fluid-fluid heat exchanger. Water is passed through the other side of the heat exchanger thus raising its temperature to either 42 °C or 83 °C. The

heated water flows to the existing hot water distribution and storage system. The heat transfer fluid leaves the heat exchanger and reenters the collector field thus completing the collection loop.

- Meanwhile, the absorption chiller produces chilled water at approximately 5 °C – 7 °C. The chilled water passes through an air-water heat exchange to produce refrigerated air.

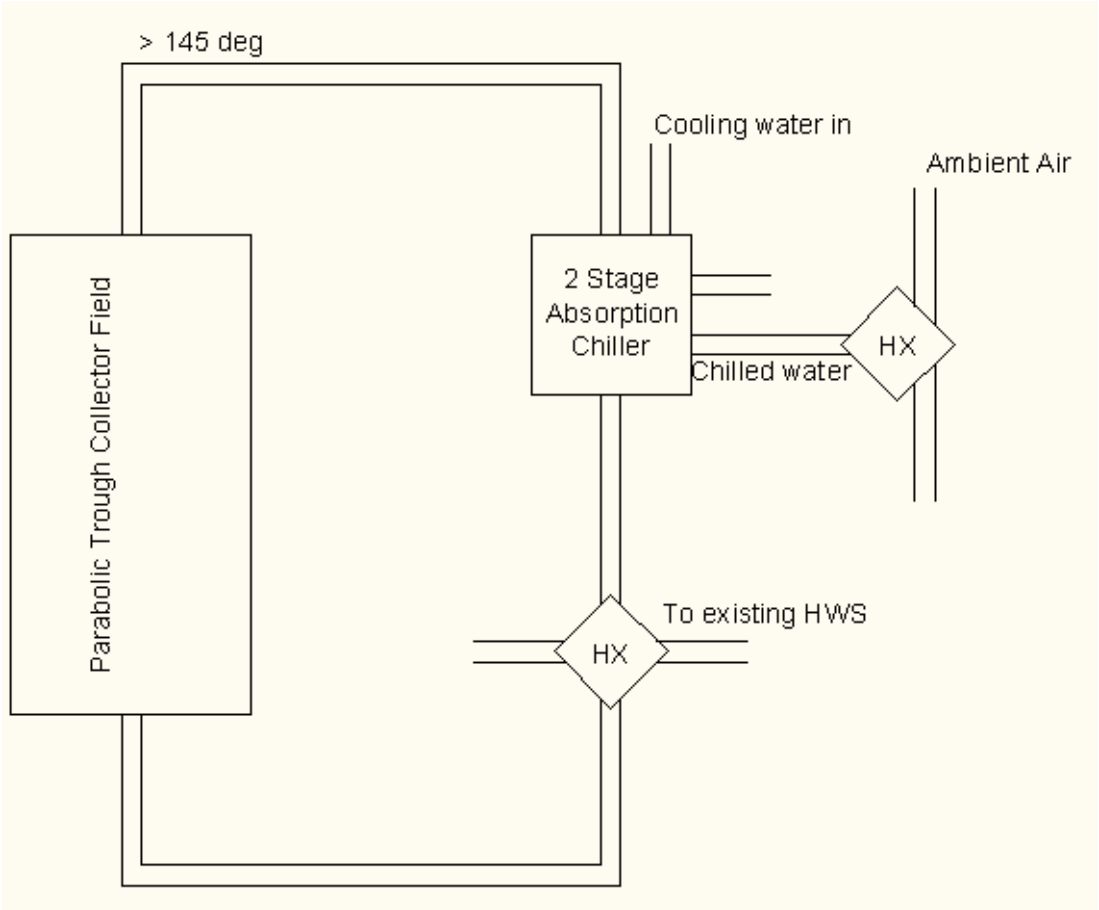

Figure 3.1 Schematic of the initial system design

3.3 Further Research into System Components

As can be seen from the previous image, the system is essentially a loop in which the output from one component in the system becomes the input to the next. As previously stated, the choice of two stage absorption cooling determined the need for the parabolic trough collectors. Now, the performance of such a collector field within the space available dictates the size of the chiller unit it can satisfy. Similarly, the outputs from the chiller unit define heat exchanger requirements. Output from the collection loop heat exchanger returns to the collection system and the cycle repeats.

Further research was required into analysis methods for each of these components and is presented below.

3.3.1 Parabolic Troughs

As described in Chapter 2, the PTC collector takes incident radiation and concentrates it on the receiver tube. Consequently the analysis of a parabolic trough system requires an optical and thermal analysis. Both of these analyses are greatly dependent collector characteristics.

Irradiance on the Collector Aperture

As mentioned in Chapter 2, concentrating collectors can only utilise direct beam radiation. Therefore the irradiance on the collector aperture is given by equation (2.26), repeated below:

The beam component is described by:

$$G_{Bt} = G_{Bn}\cos(\theta) \tag{2.26}$$

Where : G_{Bn} = direct beam radiation [W/m^2]; and

θ = incidence angle.

Optical Efficiency

Optical efficiency is given to be ratio of energy absorbed by the receiver to the energy incident on the collector aperture. Consequently it is affected by the optical properties of component materials, collector geometry and the standard of manufacture. According to Malik, M Mathur, S and Sodha M (1984) cited in Kalogiru (2009);

$$\eta_o = \rho\tau\alpha\gamma\left[\left(1 - A_f\right)\cos(\theta)\right] \tag{3.1}$$

Where: ρ = trough reflectance;

τ = transmittance of glass cover (on receiver);

α = absorptance receiver;

γ = intercept factor;

A_f = geometric factor; and

θ = incidence angle.

The designer of a parabolic trough will have access to all of these values.

Thermal Analysis

The thermal analysis of the trough receiver is used in order to determine how much energy can be captured. Useful energy can be used ultimately to find system efficiency. The receiver will lose heat through conduction, radiation and convection and these factors must be considered. In the case of receivers surrounded by a glass cover with the space between evacuated (most receivers), analysts seek to determine a loss coefficient, U_L, an overall heat loss coefficient, U_O. These terms are related to the receiver area, heat loss coefficients for convection and radiation and can be used

to find F_R, the heat removal factor. Kalogiru (2009) provides the theory behind this entire process but has not been included in this chapter as it was not used in the analysis for reasons to be explained shortly.

After completion of a thermal analysis the amount of useful energy collected is given below as:

$$Q_u = F_R[G_B\eta_o A_a - A_r U_L(T_i - T_a)] \tag{3.2}$$

Where : Q_u = useful energy [W];
F_R = heat removal factor;
G_B= incident beam radiation (equation 2.26);
η_o = optical efficiency;
A_a = aperture area [m^2];
A_r = receiver area [m^2]; and
$T_i - T_a$ = difference between inlet an ambient temperature.

Collector Performance

If equation (3.2) is divided by the total incident radiation, $G_B A_a$, the efficiency, η of the system is derived.

$$\eta = F_R\eta_o - \frac{F_R U_L(T_i - T_a)}{CG_B} \tag{3.2}$$

Where: F_R = heat removal factor;
G_B= incident beam radiation [W/m^2] (equation 2.26);
η_o = optical efficiency;
C = concentration ratio, A_r/A_a *; and*

$T_i - T_a$ = difference between inlet an ambient temperature.

Kalogiru (2009 pp. 219-226) states that in reality, the heat loss coefficient U_L described in the previous section is not constant but a function of the inlet and ambient temperatures.

Consequently,

$$F_R U_L = c_1 + c_2(T_i - T_a)$$

Therefore efficiency can be rewritten as

$$\eta = k_0 + k_1(y) - k_2 G_b y^2 \quad (3.3)$$

Where : $k_0 = F_R \eta_o$;
$k_1 = c_1/C$;
$k_1 = c_2/C$; and
$y = (T_i - T_a)$.

Through extensive testing, the producer of a PTC can eventually obtain the 2nd order polynomial to describe their collector efficiency.

The Incidence Angle Modifier, K_θ

The performance equations presented in the previous section hold true if the solar beam radiation strikes at normal to the collector aperture. When the radiation strikes off-normal the optical efficiency is affected. The higher the incidence angle the greater the impact on optical efficiency. To account for these effects the incident angle modifier (IAM) is applied to the efficiency equation as shown below;

$$\eta = K_\theta k_0 + k_1(y) - k_2 G_b y^2$$

(3.4)

Similar to the case of collector efficiency, through extensive testing the IAM for a collector can be found through the fitting of a 2nd order polynomial to recorded data.

Array design

As industrial systems typically utilise a large number of collectors to satisfy the process requirements array design becomes an important consideration for design. Kalogiru (2009), states that it is typically encouraged to arrange collectors in parallel connection; specifically in the "reverse-return array method". This array method ensures that the collector is self balancing. In other words, each collector will operate with the same flow rate and pressure drop. The collectors are plumbed such that fluid entering and leaving each module will travel the same distance; that is the first collector to be supplied is the last to return the fluid. If series connection of modules is required it should be remembered that the performance of the other modules will suffer slightly due to higher receiver temperatures which ultimately lead to greater losses. However, if the flow rate through collectors in series is adjusted (single module flow multiplied by the number in the series) the single module performance data can still be used.

NEP Solar and the PolyTrough 1200

After the discovery of the information presented above it became obvious that a sample PTC would be needed if any analysis was to be carried out for a potential field at the abattoir. At this point the search began for a company that manufactured parabolic trough collectors who would be willing to assist.

The first company found was NEP Solar, located in Warriewood, NSW. When the first phone call was made I was put in touch with Johan Dreyer who it was later learned is the CEO. After explaining the project, learning about NEP and explaining what they could do to help Johan agreed to assist in the project.

As outlined in previous sections, collector performance is affected primarily by the amount of incident radiation, the incidence angle, collector geometry and trough characteristics. Determining the useful energy that can be collected from a field of solar collectors requires the use a model that will consider all of these factors.

In order to model a collector field for the case of the abattoir NEP provided the following assistance;

- TMY data for Ipswich (an incredibly valuable piece of information)
- Whilst they would not share the methods behind their collector yield model they agreed to provide a set of their results for Ipswich in order for a comparison to be made.
- As NEP seeks to protect their intellectual property exact collector details would not be provided (such as collector geometry). They did however provide their own 2^{nd} order equations for collector efficiency and IAM.

The process of building the yield model for Ipswich is presented in a later section. The collector loop in a PolyTrough 1200 system is maintained at 16 bar and utilizes water as the working fluid. By maintaining the collector loop at high pressure, water can be heated well above boiling point (in the case of this collector up to 220 °C).

Based on collector dimensions provided in a PolyTrough 1200 brochure, the following collector array was designed with the aim of using the available space as efficiently as possible.

A 30 module array was specified; 15 rows with 2 modules per row. Each module has an aperture area, A_a of 28.2 m^2. These collectors utilise single axis tracking, repositioning themselves every 10 seconds to follow the sun.

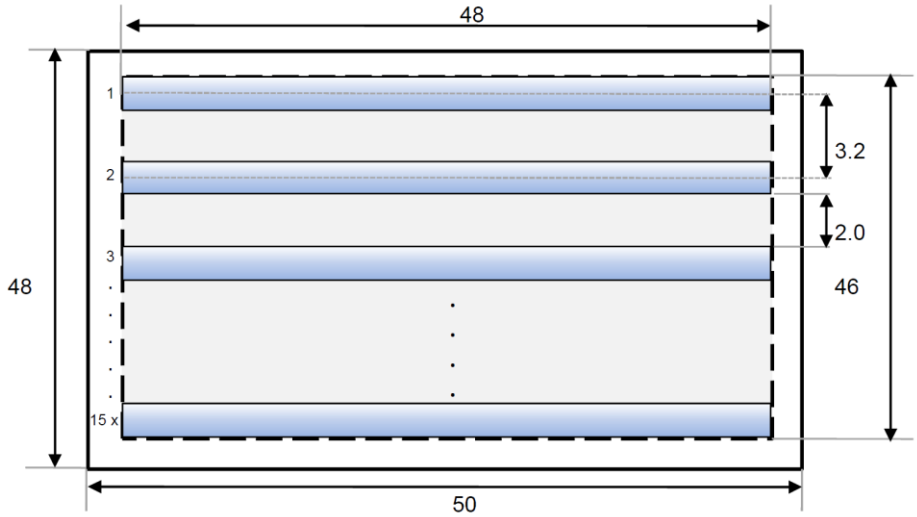

Figure 3.2 Specified collector array as drawn by NEP Solar

The rows are connected in parallel so that the pressure drop over each row is the same. Within the rows as stated previously there are two modules in series meaning the output of the first is the input to the second. This reduces system performance if not addressed. By simply doubling the flow through each row, the single collector performance data will hold true. The spacing between the two is such that shading effects are minimized.

Figure 3.3 A PolyTrough 1200 module courtesy of NEP Solar

3.3.2 Two Stage Absorption Chillers

Initially it was thought that a full system analysis of a LiBr-H_2O chiller would be conducted. Books such as Kreider, Kreith and Goswami (2000), Kalogiru (2009) and Herold, Klein and Radermacher (1996) provide methods for determining the state of the working fluid at any point in the entire cycle.

The process of analysis (to determine COP, mass balances and heat input) can be summarised as follows.

Inputs required

- Determine the amount in kW, of refrigeration required. Also specify the desired operation temperature of the evaporator, absorber and condenser and the temperature of the fluid pumped to the solution heat exchanger.
- Determine generator temperature; provided by heated fluid from the energy collection systems.

Assumptions

- For the points where temperature is specified it is assumed that refrigerant and absorbent phases are in equilibrium.
- Pressure drop in lines and internal heat exchangers are neglected. Pressure drop between condenser-absorber and solution HX return-Absorber cannot be neglected.
- The pressures in the condenser and evaporator are equal to the vapor pressure of refrigerant (water). These values can be read from a steam table. The same applies for enthalpy.
- LiBr mass fraction can be read from a LiBr concentration chart based on the values of enthalpy found in the previous step and the solution temperature.
- Mass balances are applied across key point on the system. For example across the generator;
    - Total mass balance, $\dot{m}_G = \dot{m}_1 + \dot{m}_7$.
      That is to say that mass through the generator is equal to mass returning to absorber plus mass to condenser.

- LiBr balance, $\dot{m}_G X_s = \dot{m}_1 X_{ab}$.

  This relationship shows that the concentration of LiBr in the solution returning to the absorber is higher than the input solution.

This process is repeated until the system has been fully defined.

- Eventually the rate of heat supply to the generator for the required cooling effect is found allowing calculation of COP.
- Heat transfer rates across solution exchanger and the condenser can be found using $\dot{Q}_{1-2} = (h_1 - h_2)$. The rate of heat removal from the absorber is found via a system wide heat balance; $\dot{Q}_a = \dot{Q}_{cond} - \dot{Q}_G - \dot{Q}_{evap}$

ECS and the BROAD Series Absorption chillers

Similar to the solar collection system, the methods to analyse the chiller had been found. It is likely that a chiller could have been specified on the basis of the calculations above. However it was deemed more relevant to the projects aims to source a potential chiller from industry for use in the system design.

Johan (NEP Solar) said that in the past NEP had worked on similar projects using two stage absorption chillers sourced from Energy Conservation Systems, Brisbane. He provided the name of one Shaun McKinnon. Once more, after a phone call explaining the project aims, progress thus far and what was needed to progress ECS Brisbane was on board.

When asked whether it would be worth analyzing the system using the methods outlined previously Shaun stated that nobody does that anymore. Rather their systems are designed with integrated sensors and computer control that inform the owner of all temperatures, flow rates, concentrations and so on.

ECS provided the following assistance to the project;

- The latest catalogue for the BROAD: Generation X Absorption Chillers. The catalogue provides everything from system installation and construction advice, system requirements, dimensions, and most importantly the performance data. Based on a specified temperature drop through the primary

generator a value for the power required to run the system is obtained. When the power output of the field is known a chiller is selected accordingly.

- A second data sheet showing
    - Model selection curves detailing chilled/cooling water temp, cooling capacity and COP for a specified cooling capacity. For example, if the unit is operating at 90% capacity and must produce chilled water at 6 °C then cooling water should be supplied at 30 °C. The COP is through the average of the COP values attached to the 3 values just stated.
    - Model selection curves showing the chilled/cooling water flow rates against pressure drop. For example, in a BH20 chiller the pressure drop in chilled water at 100% design flow is 30 kPa.

3.3.3 Heat Exchangers

The primary focus of the system design thus far had been the energy collection devices and the chiller. However the elements that ultimately define the system capabilities are the heat exchangers. As shown previously there are two devices needed in the system; one for a collector loop to water exchange and the other for an ambient air to chilled water exchange.

According to Shaun from ECS, the people who could provide assistance on heat exchanger sizing were Actrol Parts, Salisbury. Through this connection Ray Findlay and Claes Larsson joined the number of those assisting on the project.

3.4 Building the Solar Yield Model

Knowing the capabilities of the collector field is the key to determining system capability. As NEP Solar were not going to share their method for analysis (and had never been expected to) it was determined that a yield model should be built for an ideal collector field located in Ipswich. Due to the nature of the data it was decided that Microsoft Excel would be the modeling tool.

The model built by NEP Solar calculates all relative solar angles, radiation values and collector performance values for *every* hour of the year (as this is the format that a TMY comes in) in addition to other statistical analyses. This was deemed overly complex for the interest of this project. Rather after consultation with the supervisor Steven Goh and Johan from NEP Solar it was decided that the if the system yield for an average day of each month could be found, the monthly yield could be approximated by simply multiplying this value by the number of days in the month. Kalogiru, (2009, p. 56) provides the table below showing which day of the month should be used to provide the most accurate monthly representation. Based on the models findings, power output from the field can be found and a chiller model selected accordingly. The model does not include shading losses as they are assumed to be negligible.

Note that all tables built in the model are included in Appendix B

Table 3.3 Recommended Average Days, (Source: Kalogiru, 2009)

Month	Day Number	Average day of month		
		Date	***N***	**δ °**
Jan	*i*	17	17	-20.92
Feb	31 + *i*	16	47	-12.95
Mar	59 + *i*	16	75	-2.42
Apr	90 + *i*	15	105	9.41
May	120 + *i*	15	135	18.79
Jun	151 + *i*	11	162	23.09
Jul	181 + *i*	17	198	21.18
Aug	212 + *i*	16	228	13.45
Sep	243 + *i*	15	258	2.22
Oct	273 + *i*	15	288	-9.6
Nov	304 + *i*	14	318	-18.91
Dec	334 + *i*	10	344	-23.05

The process behind the models operation is as follows:

- Find solar position at every hour of an average day for each month. This involves calculation of AST, hour angles, solar elevation and azimuth angles and incidence angles. Described below in subsection 3.4.1.
- The hourly beam radiation for each month supplied in the TMY is averaged. In this way hourly radiation data for an average day is produced. The cosine loss is applied to the hourly insolation to give the true level of radiation incident on the collector aperture. Described below in subsection 3.4.2
- Based on the radiation incident on the collector aperture, the model finds an hourly yield using the performance equations provided by NEP Solar specific to the PolyTrough 1200. Described below in subsection 3.4.3.
- Determine yield for the average day and multiply by the number of days in the month to obtain the monthly yield. Described below in subsection 3.4.3.

3.4.1 Solar Position

There are a number of variables that must be known in order to describe the suns position at any hour of any day; these are the fundamental solar values described in Sections 2.4 – 2.9. Typically, each variable calculated is dependent on values calculated previously. This was the primary focus of the first tables built in the model.

The values calculated are outlined below, followed by sample tables from the model.

Apparent Solar Time

As solar calculations depend on AST it was the first set of data calculated. An AST value needed to be found for every hour of the day. Recall that AST is either slightly ahead or behind LST.

$$AST = LST + ET \pm 4(SL - LL) - DS \tag{2.1}$$

Where: LST =Local Standard Time
ET = Equation Time [min];
SL = Standard Longitude [degrees];
LL = Local Longitude [degrees];
DS = Daylight Savings (0 or 60) [min].

The theory behind and the methods for calculating equation time and longitude correction were presented previously. The project model finds AST for any hour of any month using the table developed below.

Table 3.4 MODEL: Time Table used to find AST

Time Table						
	Day #	**B**	**Equation time ET (min)**	**ET in time format**	**Latitude Correction in time format**	**LST**
Jan	17	-63.30	-9.49	11:50 PM	12:11 AM	5:00:00 AM
Feb	47	-33.63	-14.00	11:46 PM		6:00:00 AM
Mar	75	-5.93	-9.24	11:50 PM		7:00:00 AM
Apr	105	23.74	-0.66	11:59 PM		8:00:00 AM
May	135	53.41	3.19	12:03 AM		9:00:00 AM
Jun	162	80.11	0.37	12:00 AM		10:00:00 AM
Jul	198	115.71	-5.34	11:54 PM		11:00:00 AM
Aug	228	145.38	-3.33	11:56 PM		12:00:00 PM
Sep	258	175.05	5.78	12:05 AM		1:00:00 PM
Oct	288	204.73	14.52	12:14 AM		2:00:00 PM
Nov	318	234.40	14.39	12:14 AM		3:00:00 PM
Dec	344	260.11	5.91	12:05 AM		4:00:00 PM
						5:00:00 PM
						6:00:00 PM

As can be seen above, the table includes everything needed to find AST. Notice that in Microsoft Excel, the addition and subtraction of time values requires all values of time to be fully specified. For example, 12:00 am – 13 minutes is not allowed. Therefore the ET is entered into the table as the corresponding number of minutes either side of midnight. The same concept applies to latitude correction. A sample calculation for 11 am on the March average day is as follows;

$$AST = 11{:}00AM - 11{:}50PM + 12{:}11AM = 11{:}01{:}45AM$$

Hour Angle, *h*

Recall that hour angle is dependent on AST. Using equation 2.5a below, the hour angle is computed.

$$h = \pm 0.25\ (Number\ of\ minutes\ remaining\ until\ solar\ noon)$$

(2.5a)

The hour angle at sunset/sunrise was also found for each representative day. This allows one to check the validity of the data being calculated.

Solar Altitude Angle, α

The solar altitude angle is the angle between the horizontal plane and the suns incident rays. It is calculated for every hour using the method given below.

$$\sin(\alpha) = \cos(\varphi) = \sin(L)\cos(\delta) + \cos(L)\cos(\delta)\cos(h)$$

(2.6a)

Where: L = local latitude; values north of the equator designated as positive;
φ = solar azimuth angle [degrees];
h = hour angle [degrees]; and
δ = declination angle [degrees].

By comparing solar altitude angles at sunrise and sunset to the sunset hour angle mentioned above it is easy to visualize the relationship between the two. That is, an hour angle in excess of the sunset hour angle will produce a negative solar altitude angle meaning that the sun is below the horizon.

Solar Azimuth Angle, *z*

The solar azimuth angle is the angle formed between the sun's rays measured on the horizontal plane with respect to due North (in Southern Hemisphere) with westward angles designated as positive. Solar noon occurs when the azimuth is exactly 0°.

Solar azimuth, *z* is expressed as

$$\sin(z) = \frac{\cos(\delta)\sin(h)}{\sin(\alpha)}$$

(2.10)

Where: δ = declination angle [degrees];
h = hour angle [degrees];
α = solar altitude angle [degrees].

Solar Incidence Angle, θ

This the angle formed between the sun's rays and the normal axis of a surface. This is the most important factor calculated with regard to solar position. Recall that the greater the incidence angle, the greater the cosine loss in radiation incident on the collector aperture. Section 2.6 presented the various correlations for incidence angle with regard to the different tracking methods commonly utilised.

As previously mentioned, the collectors in this model are horizontal, tracking the sun from east to west about a north-south axis of rotation. Therefore the equation needed to find the incidence angle for any hour is (2.18) given once more below.

$$\cos(\theta) = \sqrt{\sin^2(\alpha) - \cos^2(\delta)\sin^2(h)}$$

(2.18)

Where: α = solar altitude angle [degrees];
δ = declination angle [degrees];
h = hour angle [degrees].

The Average Day

All of the values mentioned above are combined to form a table such as the one shown below.

Table 3.5 MODEL: The March Average Day

March				
Local Latitude (N)	**Local Longitude (E)**	**Standard Longitude (E)**	**Declination angle, δ (degrees)**	**hss; hsr=-hss**
-27.6154	152.7596	150	-2.39	91.23
Day Hour AST	**Solar Hour Angle, *h***	**Solar Altitude Angle, *α***	**Solar Azimuth Angle, *z***	**Incidence angle, θ**
5:01:45 AM	-104.56	-11.73	-80.99	8.82
6:01:45 AM	-89.56	1.49	-88.09	1.91
7:01:45 AM	-74.56	14.77	-84.88	4.95
8:01:45 AM	-59.56	27.89	-77.08	11.40
9:01:45 AM	-44.56	40.55	-67.32	17.04
10:01:45 AM	-29.56	52.13	-53.41	21.46
11:01:45 AM	-14.56	61.19	-31.42	24.29
12:01:45 PM	0.44	64.77	1.03	25.23
1:01:45 PM	15.44	60.77	33.00	24.17
2:01:45 PM	30.44	51.50	54.40	21.25
3:01:45 PM	45.44	39.83	67.97	16.74
4:01:45 PM	60.44	27.14	77.57	11.04
5:01:45 PM	75.44	14.00	85.30	4.56
6:01:45 PM	90.44	0.72	87.68	2.32

In examining the table above we can justify its results based on the following observations;

- Solar altitude is initially negative before rising, reaching its peak around midday and setting once more. Note the previously mentioned relationship between sunset hour angle and solar altitude. At 6:01:45PM, the hour angle is less than 91.23° and so the sun is only just up.
- Recall that negative angles of solar azimuth were designated east. Before midday solar azimuth is negative.
- It was mentioned in Chapter 2 that at solar noon, corresponding to AST = 12PM the hour angle is always zero. In the table above, just after 12PM AST the value for the hour angle is only just positive.

3.4.2 Solar Radiation Data

With the solar position fully defined relative to the collection systems, it was now necessary to determine the radiation incident on the collector aperture throughout the day.

As previously stated, NEP Solar provided TMY data for Ipswich. This was a very valuable contribution as it greatly increases the validity of the final results. An excerpt of TMY data is shown below.

Table 3.6 MODEL: TMY except courtesy of NEP Solar

Ipswich - Australia		All radiation values given in W/m^2							
-27.6154	152.7596								
3	1	6	1422	4	4	0	23.9	4.1	82
3	1	7	1423	73	67	37	24.6	3.7	82
3	1	8	1424	265	177	219	25.8	3.9	82
3	1	9	1425	393	279	191	27	4.9	82
3	1	10	1426	398	335	82	26.6	4.1	89
3	1	11	1427	735	425	354	29.2	4.9	82
3	1	12	1428	598	459	149	29.7	4.7	82
3	1	13	1429	650	427	239	30.3	6.1	79
3	1	14	1430	78	78	0	29.3	7.1	84
3	1	15	1431	67	67	0	28.5	6.8	86
3	1	16	1432	50	50	0	27.6	4.4	86
3	1	17	1433	30	30	0	27.5	3.7	82
3	1	18	1434	11	11	0	27	3.5	82

Where *G_Gh* = global (total) radiation on horizontal surface [W/m^2];
G_Dh = diffuse radiation on horizontal surface [W/m^2];
G_Bn = beam radiation [W/m^2];
T_a = ambient temperature [degrees C].
FF = wind speed [m/s]; and
RH = relative humidity.

The table shows that values are arrayed for every hour of the year in their respective vertical columns.

Recalling that a PTC can only utilise beam radiation, the model is only interested in the values of *G_Bn.* The next step was to obtain an hourly radiation profile for the average day. This was done through finding the average radiation value for each particular hour of every day over the entire month.

Such analysis for March produced the following radiation profile.

Table 3.7 MODEL: Radiation profile for the March average day

March Tracked Collector		
Day Hour	**G_Bn, W/m^2**	**Gbt, W/m^2**
6.00	0.00	0.00
7.00	237.32	236.44
8.00	486.00	476.41
9.00	589.74	563.85
10.00	588.42	547.61
11.00	621.81	566.77
12.00	565.32	511.41
13.00	568.68	518.81
14.00	564.03	525.70
15.00	565.19	541.24
16.00	558.13	547.79
17.00	447.74	446.32
18.00	199.45	199.29
19.00	0.00	0.00

Where *G_Bt* is a function of incidence angle as given below:

$$G_{Bt} = G_{Bn}\cos(\theta)$$

3.4.3 Collector Performance

It has been mentioned that NEP Solar provided the performance equations for their collectors, namely the equations for collector thermal efficiency and IAM. The constant coefficients in the equations presented below are developed through extensive performance tests on the collectors, the description of which is beyond the scope of the project.

Recall that the form of the both the efficiency and IAM equation is a 2nd order polynomial. The NEP Solar provided equations are given below.

Thermal efficiency, η

$$\eta = \frac{(G_{Bn}\eta_O - k_1\Delta T - k_2\Delta T^2)}{G_{Bn}} \tag{3.5}$$

Where: G_{Bn} = beam radiation on aperture [W/m^2];
η_o = 65 %;
k_1 = 0.4000;
k_2 = 0.0015; and
ΔT = is the temperature rise over the collector (Tin – Tout) [degrees].

Incident Angle Modifier, K_θ

$$K_\theta = a\theta^2 - b\theta - c \tag{3.6}$$

Where: a = -0.0001576;
b = -0.0009167; and
c = 1.0027789.

Notice that the equation for efficiency is dependent on the temperature change over the length of the collector. This meant that the rest of the system needed to be reasonably defined in order to estimate a reasonable temperature of fluid returned to the collector. After consultation with Johan and Shaun, it was decided that the systems performance would be evaluated for a 30 °C temperature rise over the collector. This accounted for the typical 15 °C drop in working fluid temperature as it passes through the generator of the absorption unit and a 15 °C allowance for hater heating.

Using these equations, the performance of the collector field is determined as shown in the table below. The field is comprised of 30 PolyTrough 1200 collectors, each having an aperture area of 28.2 m^2. This gives a total aperture area of 864 m^2. The temperature rise across the collectors is designed to be 30 °C.

Table 3.8 MODEL: Field performance on a March average day

PolyTrough 1200; Field; March Average Day						
hour	**Gbt w/m^2**	**Incidence Angle**	**IAM, K_θ**	**Thermal Efficiency**	**Useful energy, Qu kJ**	**Power kW**
6	0.00	1.91	1.00	0.0000	0.00	0.00
7	236.44	4.95	0.99	0.6281	459278.15	127.58
8	476.41	11.40	0.97	0.6565	945414.69	262.62
9	563.85	17.04	0.94	0.6608	1091069.04	303.07
10	547.61	21.46	0.91	0.6601	1023781.88	284.38
11	566.77	24.29	0.89	0.6610	1034175.58	287.27
12	511.41	25.23	0.88	0.6584	920996.28	255.83
13	518.81	24.17	0.89	0.6588	944594.74	262.39
14	525.70	21.25	0.91	0.6591	983089.12	273.08
15	541.24	16.74	0.94	0.6599	1047821.60	291.06
16	547.79	11.04	0.97	0.6601	1094912.31	304.14
17	446.32	4.56	1.00	0.6546	904502.58	251.25
18	199.29	2.32	1.00	0.6175	382709.98	106.31
19	0.00	0.00	1.00	0.0000	0.00	0.00
				Total, kJ	10832345.95	
				Power kWh	3008.98	

Chapter 4 –Yield Model Results and Design Refinement

4.1 Introduction

This chapter presents the results of the solar yield model developed previously. It has been previously stated that the performance of the system dictates the requirements of the other components within the system. Based on the results of the yield model the initial design can be re-evaluated. Knowing the collectors capabilities allows the selection of an absorption chiller and initial sizing of heat exchangers. Once this has been done and their capabilities defined the initial design phase in complete.

4.2 Yield Model Results

The modeling process outlined in Chapter 3 was repeated for every month. Once the collector yield had been determined for the average day of each month, the value was multiplied by the number of days in the month. This validity of this assumption was approved by both Steven and Johan.

When all yield data was available it was determined that an array of 30 PolyTrough 1200 collectors at an Ipswich site would have an annual yield of approximately 864 MWh.

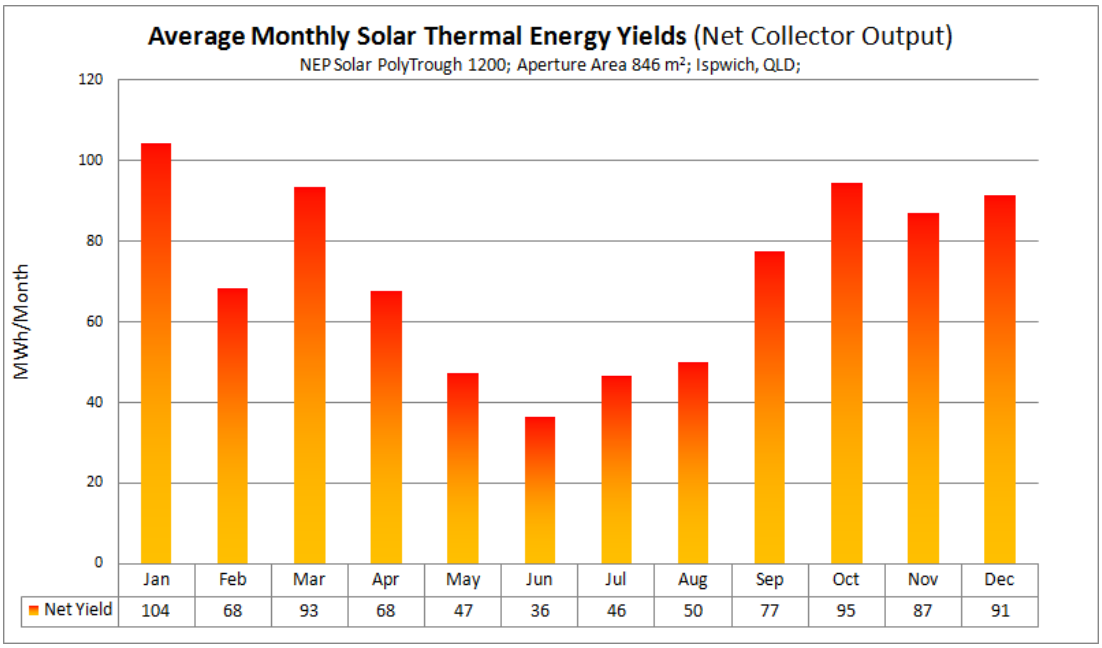

Figure 4.1 The Model Results for Collector Yield

At this stage, NEP Solar provided the results of their own yield analysis for Ipswich as promised. Their result is displayed below.

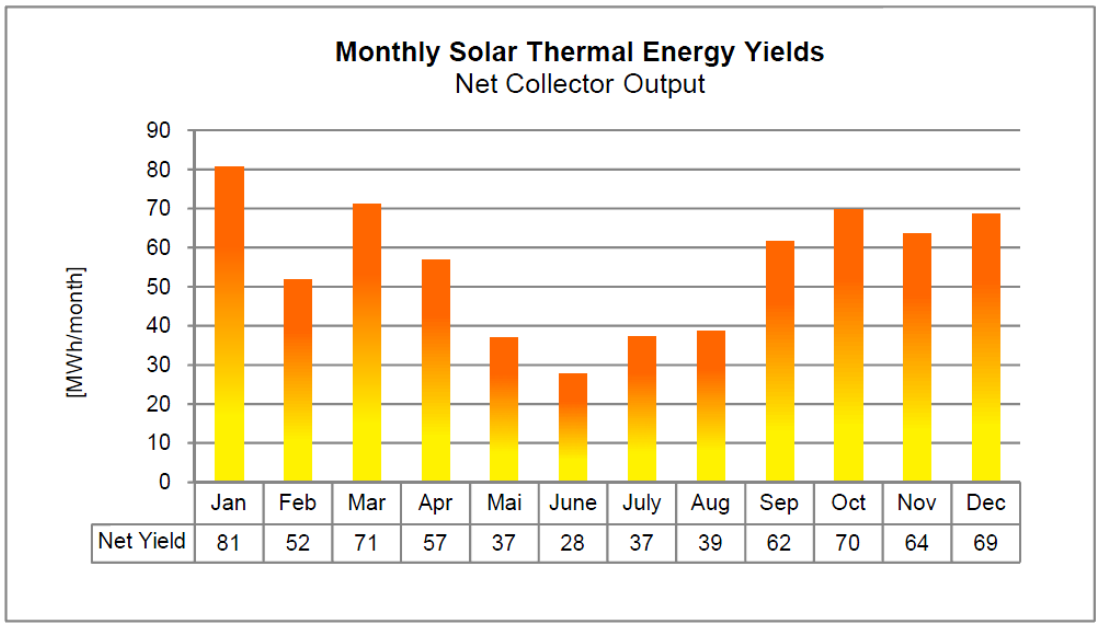

Figure 4.2 Collector Yield Predicted by NEP Solar

When comparing the results of the two models it is seen that the yield model produced in the previous chapter provides a similar yield profile to that of NEP Solar. Remember that NEP Solar did not share the theory or method behind their model. In essence this is a verification of the methods used to build the projects model as described in Chapter 3.

On closer inspection it is revealed that the project model predicts a higher yield for every month of the year and hence a higher annual yield. The table given below was constructed to allow comparison of yield values and to determine the system error.

Table 4.1 Model Error

Model Predicted Monthly Collector Yields			**NEP Solar Model Yields**		**Error of model as compared to NEP**
Month	**MWh**		**MWh**		**Error**
Jan	104		81		0.222884
Feb	68		52		0.240188
Mar	93		71		0.238839
Apr	68		57		0.158286
May	47		37		0.215226
Jun	36		28		0.230914
Jul	46		37		0.203569
Aug	50		39		0.220031
Sep	77		62		0.199229
Oct	95		70		0.260139
Nov	87		64		0.263386
Dec	91		69		0.244015
Annual Yield	864		655		0.241787

The project model provides an over estimate of monthly yield by approximately 22%. Over the course of the year this error leads to overestimation by almost a quarter. After considerable thought, and consultation with Johan the following conclusion was drawn as to the reason for the discrepancy.

The general profile of the results is the same meaning that the solar position calculations remain valid. Whilst the processes behind his model were not shared, Johan did state that the NEP Solar yield model calculates collector performance at *every* hour of the TMY. This means that for every hourly radiation entry in the TMY, individual values of apparent solar time, declination, hour angle, solar elevation, solar azimuth and incidence angle have been previously defined. When compared to the method behind the project model (finding an average day for each month based on its monthly radiation profile, multiplying daily yield out to a monthly yield) it is believed that the error is induced through the averaging of radiation data. This is the only area on which the two models differ. It is quite conceivable that the small error induced through the process of averaging the radiation profile for a single day is increased dramatically when the results are applied to the entire month. However, as the results provided by NEP Solar only give a total monthly yield, a comparison between errors on a daily basis could not be carried out.

The full results of the NEP Solar yield model are presented in Appendix C. As mentioned above, their model analysed each and every hour of the year. This method also becomes more accurate when attempting to determine the peak power output by the system. To further explain this concept, consider a day in January where the incident radiation at midday is 1042 W/m^2. Due to the effect of cloudy days and other meteorological issues the incident radiation for the same hour in the average day is found to be 676 W/m^2. Consequently the model will under estimate the power output that can be provided by the collector under such high level insolation.

As the model could not predict the actual peak power for the field, it was deemed reasonable to use the NEP Solar results for the remainder of the system design. Although the project designed yield model was not entirely accurate, it was however a valuable learning process. In this light the model may be viewed as successful. The model represents the consolidation of theory presented in a number of texts (and outlined here in previous sections) in order to produce a yield model unique to the project, with no guidance as to the process behind doing so received. Error in predicted values aside, the fact that the same monthly yield profile is produced between the project and NEP Solar models can be seen as a validation of the process used in all areas except the treatment of radiation data.

NEP Solar provided the following frequency distribution showing the collectors thermal output over the year.

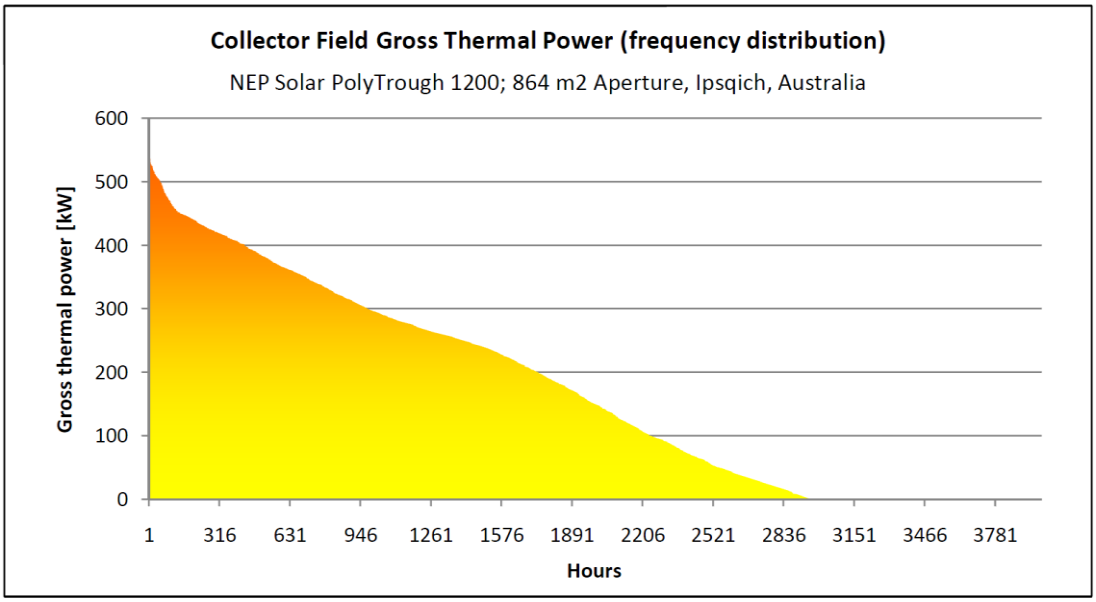

Figure 4.3 Gross thermal power, frequency distribution

It shows that field has a peak power output of 518 kW. With the collector performance determined the process of refining the design can begin.

4.3 Design Refinement

4.3.1 Chiller Selection

It was mentioned previously that Shaun from ECS Brisbane provided technical information on the BROAD series of absorption chillers that they provide and install. This information provided the means by which to determine an appropriate chiller

for the system as well as the performance it could deliver. The image below shows one of the key tables given in the catalogue.

Table 4.2 An excerpt from the BROAD catalogue

Packaged Waste Heat Chiller (Hot Water Chiller) Performance Data
jacket water from generator and industrial waste hot water
(pump set, cooling tower, machine room's data as the same as DFA)

code	model	cooling capacity	chilled w.		cooling W.		hot water cons-umption	power demand	solution weight	unit ship. wt.	chiller ship. Wt.	unit operation weight
			flowrate	pressure drop	flowrate	pressure drop						
		kW	m^3/h	kPa	m^3/h	kPa	m^3/h	kW	t	t	t	t
two-stage hot water chiller BH hot water 180°C	20	233	28.5	30	48.8	50	10.3	1.7	0.98	3.3	/	4.7
	50	582	71.3	30	122	50	25.7	4.3	2.2	5.8	/	8.7
	75	872	107	30	183	50	38.5	4.6	2.8	7	5.4	11.1
	100	1163	142	30	244	50	51.4	6.8	3.4	9.3	7	13.7
	125	1454	178	30	305	50	64.2	6.8	4.4	10.7	8.3	16.1
	150	1745	214	40	366	50	77.1	6.8	4.9	11.9	9.2	18.6
	200	2326	285	40	488	50	103	10.2	7.1	15.2	12	24.7
	250	2908	356	50	610	60	128	10.2	7.8	19.3	14.5	31.6
	300	3489	427	50	733	60	154	11.7	10.6	21.5	16.3	36.7
	400	4652	570	50	977	60	206	13.2	12.1	/	21.3	46.6
	500	5815	712	60	1221	70	257	17.7	14.8	/	25.9	53.3
	600	6978	854	60	1465	70	308	20.7	18.1	/	29.9	64.7
	800	9304	1139	60	1953	70	411	25.9	24.2	/	38.3	81.4
	1000	11630	1429	60	2442	70	514	34.9	30.5	/	37.5	97.0

This table provides information on all of the 2 stage chillers driven by hot water (as opposed to steam or natural gas) within the series. In order to determine the size of the unit best suited for the design, a figure for power consumption in the generator needed to be found.

Based on a temperature drop of 15 °C in the loop water (informed by Shaun that this value is a common design assumption when dealing with this equipment) as it passes through the generator the following analysis was used to determine power consumption.

$$Q_G = \dot{m} c_p \Delta T \tag{4.1}$$

Where: $\dot{m}$ = mass flow rate [m^3/h];

c_p = average specific heat [J/kg-K]; and

ΔT = is the temperature drop through the generator [Kelvin].

When applied to the first three chillers in the series the results are as below.

BH20

$$Q_G = \frac{2.559 \times 4354.375 \times (15)}{1000} \approx 167\ kW$$

BH50

$$Q_G = \frac{6.385 \times 4354.375 \times (15)}{1000} \approx 417 kW$$

BH75

$$Q_G = \frac{9.565 \times 4354.375 \times (15)}{1000} \approx 625\ kW$$

Recall that the peak power output of the field is 518 kW. Shaun advised regarding model selection, to select a chiller that will best be able to utilise the available power.

In reference to the results produced above the BH75, if supplied by the field could never run at full load as the peak power never exceeds 518 kW. The BH20 would be considerably over supplied with power and some form of heat storage would need to be included. Ultimately the model selected is then the BH50. When the power exceeds 417 kW the machine performs above 100% capacity.

Now that a chiller had been selected based on its heating requirements the rest of the values surrounding it operation needed to be determined. Cooling towers to suit application are assumed to be installed as part of the chiller package. From the data

sheets provided, the chiller system has the following characteristics when operating at full load to produce chilled water at 6 °C.

BH50

Cooling capacity;	582 kW
Chilled water;	
Flow rate;	71.3 m^3/h
Temperature;	6 °C
Cooling water;	
Flow rate;	48.8 m^3/h
Temperature;	27.8 °C
COP;	1.4

4.3.2 Heat Exchanger Requirements

With the collector output specified and an absorption chiller selected all that remained was to size the systems heat exchangers. As mentioned previously there were two unit required; one for water-water exchange and the other an air-water exchange.

During initial discussions regarding the system design with Shaun, he mentioned that when the time came I should speak to Ray Findlay of Actrol Parts, Salisbury.

As a result of initial discussions with Ray regarding the heat exchange requirements of the system, it was agreed that once the operational parameters for the heat exchangers could be provided, Actrol would attempt to provide a heat exchanger that would satisfy the need. Based simply on the system requirements outlined, Ray proposed the use of compact plate heat exchangers for both units. Compact exchangers were selected due primarily for their efficiency due to the large exchange surface but also because space constraints in the abattoir would be likely.

In determining the heat exchanger requirements some engineering decisions needed to be made regarding the selection of the heat load. For example water leaving the absorber generator approaches the water-water heat exchanger with a defined temperature and flow rate. The temperature of this water as it leaves the heat exchanger needs to be defined if the heat load is to be fully defined. The same applies to the air-water heat exchange.

Based on assumed summer values of ambient temperatures (as summer is essentially the worst case for refrigeration), the initial heat exchanger requirements were defined as follows.

Table 4.3 Heat exchanger 1, initial heat load

HX 1; Water-Water		
	Side 1	Side 2
T_{in} °C	165	26
T_{out} °C	150	42
$\dot{m}$ m^3/h	25.7	
Heat Load	422.1 kW	

Table 4.4 Heat exchanger 2, initial heat load

HX 2; Air-Water		
	Side 1	Side 2
T_{in} °C	35	6
T_{out} °C	10	13
$\dot{m}$ m^3/h		71.3
Heat Load	581 kW	

Heat Exchanger 1 – Water-Water

Ray passed the heat exchange requirements onto Claes Larsson, one of the engineers at SWEP heat exchangers. Claes would input the duty requirements of the heat exchangers into the companies sizing program and provide a unit to satisfy the need.

However, the initial outputs of the program based on the requirements above produced an unacceptable system. There was a pressure drop in both fluid streams of almost 50 kPa and an 820% over surfacing factor. Over the phone Claes explained that this was due to the high flow rate of the hot stream and the relatively low temperatures on the other side.

In order to produce a reasonable heat exchanger it was decided that the output temperature of the secondary stream, previously defined to be 42 °C would now be increased to 84 °C. The heat load would remain the same, hence flow rate and outlet temperature of the heated water would need to be reduced. The inclusion of a by-pass loop in the collector line with a flow limiter was proposed to achieve this.

Upon reevaluation of the system requirements as outlined above it was concluded that a SWEP B10Tx46H/1P compact brazed heat exchanger could produce water at 84 °C for use in the abattoir at a rate of 6345 L/h. Water in the collector bypass loop exits the exchanger at 50 °C before rejoining the primary loop.

Heat Exchanger 2 – Air-Water

Again, Ray passed the heat exchange requirements onto Claes. The results of the companies program showed that the compact heat exchangers were totally unsuited to an air-water exchange, primarily because the air would need to be compressed for and reasonable heat removal. For example, one air-water option sized by the system consisted of 100 heat exchangers in parallel connection.

The compact exchanger concept was ruled out. Instead, an air duct/coil option was proposed. In this case a duct is specified and a coil through which the chilled water is passed is placed within. A fan is placed in the duct, either before or after the coil to

draw air through the system. As the air is forced over the coil it surrenders its heat and is ducted away.

Once this decision was made I set about conducting a preliminary analysis of such a cooling system. Air will enter the duct at atmospheric pressure, 35 °C @ 60% relative humidity (assumption for worst case scenario; summer will have the highest ambient temperature and thus the highest cooling load). The rate at which the air is fan forced through the duct is yet to be specified. Chilled water from the absorption chiller flows through a coil (or is supplied to a series of coils) that are placed in the duct. Water is supplied at 6 °C at a rate of 71.3 m^3/h, (19.8 kg/s based on a density of 999.94 kg/m^3 interpolated from water table in Bohn and Kreith (2001)). Based on these basic inputs a simple cooling analysis was conducted according to the process set out by Boles and Çengel (2007).

Data

Water in: 6 °C Air on: 35 °C @ 65% RH

Water out: 15 °C Air off: 10 °C (saturated)

Assumptions

1. A steady flow of air is supplied (constant air mass flow rate);
2. Dry air and water vapor are treated as ideal gasses; and
3. Energy changes in the system are negligible.

Working

Through the use of a psyhcometric chart (shown in Appendix E), the specific volume of the incoming air and the enthalpy drop between the inlet and exit states are determined to be;

$$v = 0.908\ \frac{m^3}{kg}\ (@\ 35\ ℃\ dry\ bulb)$$

$$\Delta h = 70\ \frac{kJ}{kg}$$

The specific heat of water is interpolated from the water table provided in Bohn and Kreith (2001) to be;

$$c_p = 4195.4 \frac{kJ}{kg}$$

Now, cooling capacity of the water in the system is found below;

$$Q_w = \dot{m}_w c_p \Delta T$$

$$Q_w = 19.80 \times 4195.4 \times 9 = 748\ kW$$

According to the concept of a system energy balance, the heat energy gained by the water is equal to the heat energy lost by the air as it flows through the system.

Therefore, applying this concept;

$$Q_a = \dot{m}_a \Delta h$$

$$\dot{m}_a = \frac{748}{70} = 10.68\ kg/s$$

Now in the case of air, with $\dot{V}$ representing volumetric flow rate;

$$\dot{m}_a = \frac{\dot{V}}{v}$$

$$\dot{V} = \dot{m}_a \times v = 10.68 \times 0.908$$

$$\dot{V} = 9.70\ \frac{m^3}{s}$$

Note that these are preliminary calculations and are included to demonstrate a basic technique for an initial duct/coil design. These calculations are based on a single duct with a single coil through which all supplied water flows. In reality it may be more

feasible to supply water to a number of individual coils in separate duct systems but this is yet to be examined.

Once the volumetric air flow has been determined and a maximum air velocity stated, one can use a generic duct calculator (a type of slide rule estimate) to determine duct sizing and friction loss. According to Ray from Actrol Parts, this is a general approach taken to such initial estimates within industry.

4.4 The Final Design

4.4.1 Summary of System Operation

The collector field proposed for the abattoir consists of 30 PolyTrough 1200 collectors utilizing E-W solar tracking. Such a field is capable of producing up to 518 kW and providing 655MWh per annum. The water within the receivers is heated, under pressure to 180 °C. This heat is used in the generator of a BROAD BH50 two stage absorption chiller. Water leaves the generator at 165 °C and the majority of this is piped directly back to the collectors. However some of the fluid enters a bypass loop with heavy flow restriction. This bypass loop provides the hot stream for a SWEP B10Tx46H/1P compact brazed heat exchanger. In this way, ambient water is heated to 84 °C for use in the abattoir at a rate of 6345 L/h. Meanwhile, the BH50 also produces chilled water at a rate of 71.3 m^3/h. The chilled water is passed though a coil within a duct through which ambient air is forced. Though there has been no initial sizing of the duct, coil or fan, there is the potential for 748 kW of cooling.

As a result of the system reevaluation the initial schematic presented earlier is modified to show the need for the bypass loop about the water-water heat exchanger.

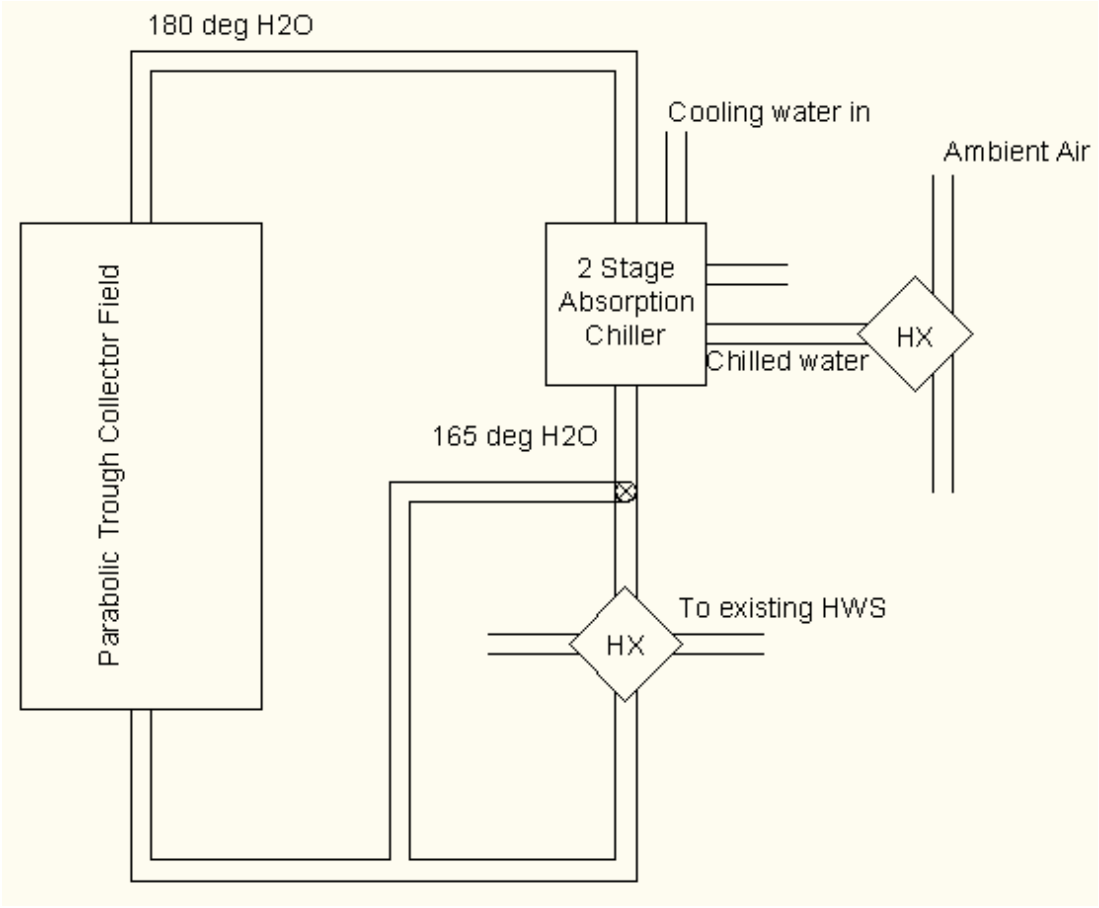

Figure 4.4 Simplified schematic of final design

Chapter 5 – Project Conclusion

5.1 Discussion

This primary aim of this project was to investigate the potential for a solar thermal system that would provide both refrigeration and water heating to Ipswich's Churchill Abattoir. Based on the generic research regarding the potential system components a conceptual system consisting of parabolic trough collectors, a two stage absorption chiller and two separate heat exchange devices was proposed.

Further research into the issues surrounding the systems mentioned above was carried out to provide deeper understanding of their performance capabilities and the way they interact dependently within the system. The process of seeking proof of concept through a theoretical analysis eventually led to the selection and sizing of some components for a real system with real, defined outputs. Where components were not fully defined the elements for analysis are present but time ran short. The projects eventual involvement with industry was rewarding not only for the outcomes of the project but also in terms of personal growth and networking.

The solar yield model built in order to determine potential collector yield for an array in Ipswich, whilst not explicitly used in the final design stages was still a very relevant system. It showed the same monthly yield profile as the results produced by NEP Solar. Bearing in mind that none of the theory behind their own model was shared beyond the equations for collector efficiency and incident angle modifier, this was very promising. As discussed in Chapter 4 it is believed the model was let down by its treatment of radiation data

Based on the findings of this project it can be concluded that the Churchill Abattoir could stand to benefit considerably through the implementation of such a system. Indeed the applications for a system such as this spread far beyond the meat processing industry to any situation where relatively low levels of refrigeration are required.

5.2 Future Work

Future work in completing this design project includes

- Modification of the project built solar yield model to calculate collector performance for every value in the TMY data. This should see a significant reduction in errors between the project model results and those provided by the industry model.
- Design of the air-water heat exchange component. The initial concept is for a fan driven air duct in which air is forced through a coil containing chilled water produced by the absorption chiller. Further work is needed to adequately define potential performance as well as duct, coil and fan sizing.
- There is also the need for greater mechanical design beyond a successful conceptual study; re evaluation of the air cooling system, design of system piping and instrumentation, structural support, control systems/monitoring etc.
- Once the entire design process is complete a cost/benefit analysis can begin to determine installation costs, energy savings, payback period and so on.

5.3 Recommendations

If management at Churchill Abattoir is seriously considering the application of such technology to their operations it is recommended that they approach industry as soon as possible. More than once this project was subjected to delay as those providing assistance were too busy with their own responsibilities.

All of the industry connections in this project arose through the recommendations of Johan Dreyer, CEO of NEP Solar. Essentially he provided contact details for the companies they use when designing their solar thermal systems.

NEP Solar – 0266 9998 4700 or contact@nep-solar.com. Ask for Johan and mention this project.

References

Australian Industry Group, n.d. *"Saving energy in meat processing facilities*", PDF, retreived May 2010, <http://pdf.aigroup.asn.au/environment/24_Meat_Processing_Abattoir_Energy_Reduction_Factsheet.pdf>

Aye, L and Fuller, R 2007, *Seasonal storage for solar thermal systems in Australia*, accessed May 2010, <http://www.deakin.edu.au/dro/eserv/DU:30007947/fuller-seasonalstorage-2007.pdf>

Beckman, W and Duffie, J, 1991, *Solar engineering of thermal processes*, John Wiley and Sons, New York

Bohn, S and Kreith, F 2001, *Principles of heat transfer*, 6th edn. Thomson, Toronto

Boles, M and Çengel, Y 2007, *Thermodynamics: An engineering approach*, 6th edn. McGraw Hill, New York

DDC Energy Services, 2007, *Cogen in the abattoir*, accessed May 2010, < http://www.ddcenergy.com.au/DDCES_assets/EcoGeneration_Mar_Apr_2007_Full.pdf>

Department of Primary Industry Victoria, 2010, *Biogas*, accessed May 2010 < http://new.dpi.vic.gov.au/energy/future-energy/transport-energy/victorias-current-and-alternative-transport-fuels/biogas>

Dept. of the Environment, Climate Change and Water, 2008, *Environmental issues – abattoirs*, accessed May 2010, <http://www.environment.nsw.gov.au/mao/abattoirs.htm>

Ecogeneration, 2010, *Cogeneration plant lowers emissions at Midfield Meats*, vol. 56 Jan/Feb

Energy Solutions Centre, 2008, digital image, Gas fired air conditioning equipment, Energy Solutions Centre, accessed May 2010, <http://www.gasairconditioning.org/absorption_how_it_works.htm>

GreenSpec, n.d, *Solar hot water collectors*, digital image, GreenSpec, accessed September 2010, <http://www.greenspec.co.uk/solar-collectors.php>

Herold, K Klein and Radermacher R 1996, *Absorption chillers and heat pumps*, CRC Press, New York

HubPages 2010, *How solar hot water systems work*, digital image, HubPages, accessed 10 September 2010, <http://hubpages.com/hub/Solar-Hot-Water-Systems>

Kalogiru, S 2004 "Solar thermal collectors and applications", *Progress in Energy and Combustion Science*, vol. 30, no. 3, pp. 231-295.

Kalogiru, S 2009, *Solar Energy Engineering*, 1st edn, Elesvier, San Diego

Kreider, J Kreith, F and Goswami, D 2000, *Principles of solar engineering*, 2nd ed, Taylor and Francis, Philadelphia

Meat and Livestock Australia, 1998, *Best practice wastewater treatment – wastewater manual*, accesed May 2010, <http://www.mintrac.com.au/files/diploma/Best%20practice%20wastewater%20treatment.pdf>

National Renewable Energy Laboratory, 2010, *Parabolic trough solar field technology*, digital image, National Renewable Energy Laboratory, accessed 10 May 2010, <http://www.nrel.gov/csp/troughnet/solar_field.html>

Quanshing, V 2005, *Understanding renewable energy systems*, Bath Press, Bath

Solair 2009, *Adsorption Chillers*, digital image, Solair, accessed August 2010, <http://www.solair-project.eu/142.0.html>

Solar and wind energy, 2010, digital image, accessed September 2010, <http://www.solar.net.cn/evacuated-tube-solar-collector.html>

The Minister for Regional and Rural Development, 2009, *$900,000 grant helps abattoir cut emissions*, accessed May 2010, <http://www.premier.vic.gov.au/component/content/article/5904.html>

Biblography

This list of books is intended to provide any interested parties with a starting point from which to build their knowledge. It includes the books found most useful to the project even if not specifically referenced.

Beckman, W and Duffie, J, 2006, *Solar engineering of thermal processes*, 3rd ed., John Wiley and Sons, New York

Eicker, U 2003, *Solar technologies for buildings*, John Wiley and Sons, Sussex

Herold, K Klein and Radermacher R 1996, *Absorption chillers and heat pumps*, CRC Press, New York

Hesselgreaves, J 2001, *Compact heat exchangers: selection, operation and design*, Elseveir, New York

Hoogendoorn, C Kreider, J and Kreith, F 1989, *Solar design: components, systems and economics*, Hemisphere Publishing Corporation, USA

Kalogiru, S 2009, *Solar Energy Engineering*, 1st edn, Elesvier, San Diego

Kreider, J Kreith, F and Goswami, D 2000, *Principles of solar engineering*, 2nd ed, Taylor and Francis, Philadelphia

Sorenson, B 2000, *Renewable Energy: Its physics, engineering, environmental impacts, economics and planning*, 2nd edition, Academic Press, London

University of Southern Queensland
Faculty of Engineering and Surveying

Appendix A – Project Specification

ENG 4111/4112 Research Project
PROJECT SPECIFICATION

FOR: **ZACH MULLER**

TOPIC: INVESTIGATION OF SOLAR THERMAL ENERGY ALTERNATIVES AND THEIR APPLICATIONS TO WATER HEATING AND AIR COOLING SYSTEMS IN THE MEAT PROCESSING INDUSTRY

SUPERVISORS: Steven Goh (University of Southern Queensland)
Mike Spence (Churchill Abattoir)

ENROLMENT: ENG 4111 – S1, ONC, 2010

ENG 4112 – S2, ONC, 2010

PROJECT AIM: This project seeks to investigate current solar thermal energy systems and their application to sustainable water heating and air conditioning within the meat processing industry.

SPONSORSHIP: Churchill Abattoir

PROGRAMME: **Issue A, 21st March 2010**

1. Research current alternatives in solar thermal systems
2. Research the current state/extent of alternative energy use in the meat processing industry
3. Establish design parameters
4. Produce a conceptual solar thermal system
5. Investigate the potential of such a system to cooling processes
6. Submit findings as an academic dissertation

As time permits

7. Conduct a cost analysis/feasibility study for such a system

AGREED:

_____ (student)

_____ (supervisor)

Examiner/Co-examiner: _____

Appendix B – The Solar Model

Average Days

Jan				
Local Latitude (N)	**Local Longitude (E)**	**Standard Longitude (E)**	**Declination angle, δ (degrees)**	**hss; hsr=-hss**
-27.6154	152.7596	150	-20.92	101.35
AST	**Solar Hour Angle, *h***	**Solar Altitude Angle, α**	**Solar Azimuth Angle, *z***	**Incidence angle, θ**
5:01:30 AM	-104.63	-2.49	-64.78	25.19
6:01:30 AM	-89.63	9.84	-71.45	18.27
7:01:30 AM	-74.63	22.64	-77.39	11.63
8:01:30 AM	-59.63	35.73	-83.11	5.59
9:01:30 AM	-44.63	48.99	-89.29	0.47
10:01:30 AM	-29.63	62.25	-82.59	3.44
11:01:30 AM	-14.63	75.10	-66.49	5.89
12:01:30 PM	0.38	83.29	3.00	6.70
1:01:30 PM	15.38	74.48	67.78	5.81
2:01:30 PM	30.38	61.59	83.09	3.28
3:01:30 PM	45.38	48.32	88.95	0.70
4:01:30 PM	60.38	35.07	82.82	5.87
5:01:30 PM	75.38	21.99	77.10	11.95
6:01:30 PM	90.38	9.21	71.13	18.61

Feb				
Local Latitude (N)	**Local Longitude (E)**	**Standard Longitude (E)**	**Declination angle, δ (degrees)**	**hss; hsr=-hss**
-27.6154	152.7596	150	-13.33	97.00
Day Hour AST	**Solar Hour Angle, *h***	**Solar Altitude Angle, α**	**Solar Azimuth Angle, *z***	**Incidence angle, θ**
4:57:00 AM	-105.75	-7.31	-70.77	19.07
5:57:00 AM	-90.75	0.44	-76.66	13.34
6:57:00 AM	-75.75	13.72	-76.13	13.46
7:57:00 AM	-60.75	26.87	-72.13	15.89
8:57:00 AM	-45.75	39.57	-64.73	19.21
9:57:00 AM	-30.75	51.28	-52.68	22.29
10:57:00 AM	-15.75	60.62	-32.58	24.42
11:57:00 AM	0.75	64.76	1.71	25.22
12:57:00 PM	14.25	61.33	29.95	24.56
1:57:00 PM	29.25	52.35	51.11	22.55
2:57:00 PM	44.25	40.80	63.77	19.55
3:57:00 PM	59.25	28.16	71.54	16.21
4:57:00 PM	74.25	15.05	75.88	13.62
5:57:00 PM	89.25	1.77	76.77	13.22

March				
Local Latitude (N)	**Local Longitude (E)**	**Standard Longitude (E)**	**Declination angle, δ (degrees)**	**hss; hsr=-hss**
-27.6154	152.7596	150	-2.39	91.23
Day Hour AST	**Solar Hour Angle, *h***	**Solar Altitude Angle, α**	**Solar Azimuth Angle, *z***	**Incidence angle, θ**
5:01:45 AM	-104.56	-11.73	-80.99	8.82
6:01:45 AM	-89.56	1.49	-88.09	1.91
7:01:45 AM	-74.56	14.77	-84.88	4.95
8:01:45 AM	-59.56	27.89	-77.08	11.40
9:01:45 AM	-44.56	40.55	-67.32	17.04
10:01:45 AM	-29.56	52.13	-53.41	21.46
11:01:45 AM	-14.56	61.19	-31.42	24.29
12:01:45 PM	0.44	64.77	1.03	25.23
1:01:45 PM	15.44	60.77	33.00	24.17
2:01:45 PM	30.44	51.50	54.40	21.25
3:01:45 PM	45.44	39.83	67.97	16.74
4:01:45 PM	60.44	27.14	77.57	11.04
5:01:45 PM	75.44	14.00	85.30	4.56
6:01:45 PM	90.44	0.72	87.68	2.32

April				
Local Latitude (N)	**Local Longitude (E)**	**Standard Longitude (E)**	**Declination angle, δ (degrees)**	**hss; hsr=-hss**
-27.6154	152.7596	150	9.49	85.06
Day Hour AST	**Solar Hour Angle, *h***	**Solar Altitude Angle, α**	**Solar Azimuth Angle, *z***	**Incidence angle, θ**
5:10:20 AM	-102.42	-15.33	-87.16	2.74
6:10:20 AM	-87.42	-2.12	-80.39	9.60
7:10:20 AM	-72.42	10.81	-73.18	16.51
8:10:20 AM	-57.42	23.22	-64.73	23.10
9:10:20 AM	-42.42	34.66	-53.98	28.92
10:10:20 AM	-27.42	44.37	-39.45	33.50
11:10:20 AM	-12.42	50.99	-19.69	36.34
12:10:20 PM	2.58	52.81	4.22	37.08
1:10:20 PM	17.58	49.17	27.11	35.59
2:10:20 PM	32.58	41.30	44.99	32.10
3:10:20 PM	47.58	30.87	58.03	27.03
4:10:20 PM	62.58	19.02	67.84	20.90
5:10:20 PM	77.58	6.40	75.76	14.15
6:10:20 PM	92.58	-6.65	82.74	7.21

May				
Local Latitude (N)	**Local Longitude (E)**	**Standard Longitude (E)**	**Declination angle, δ (degrees)**	**hss; hsr=-hss**
-27.6154	152.7596	150	18.81	79.90
Day Hour AST	**Solar Hour Angle, *h***	**Solar Altitude Angle, α**	**Solar Azimuth Angle, *z***	**Incidence angle, θ**
5:14:11 AM	-101.45	-18.42	-77.92	11.45
6:14:11 AM	-86.45	-5.60	-71.68	18.23
7:14:11 AM	-71.45	6.74	-64.65	25.16
8:14:11 AM	-56.45	18.31	-56.20	31.88
9:14:11 AM	-41.45	28.63	-45.56	37.92
10:14:11 AM	-26.45	36.98	-31.86	42.73
11:14:11 AM	-11.45	42.27	-14.72	45.70
12:14:11 PM	3.55	43.45	4.63	46.35
1:14:11 PM	18.55	40.23	23.22	44.56
2:14:11 PM	33.55	33.34	38.77	40.64
3:14:11 PM	48.55	23.95	50.92	35.18
4:14:11 PM	63.55	12.96	60.42	28.76
5:14:11 PM	78.55	0.98	68.11	21.89
6:14:11 PM	93.55	-11.61	74.70	14.98

June				
Local Latitude (N)	**Local Longitude (E)**	**Standard Longitude (E)**	**Declination angle, δ (degrees)**	**hss; hsr=-hss**
-27.6154	152.7596	150	23.08	77.33
AST	**Solar Hour Angle, h**	**Solar Altitude Angle, α**	**Solar Azimuth Angle, z**	**Incidence angle, θ**
6:11:22 AM	-87.16	-8.12	-68.15	21.62
7:11:22 AM	-72.16	3.90	-61.37	28.55
8:11:22 AM	-57.16	15.09	-53.18	35.35
9:11:22 AM	-42.16	25.00	-42.95	41.56
10:11:22 AM	-27.16	32.93	-30.02	46.61
11:11:22 AM	-12.16	37.97	-14.23	49.84
12:11:22 PM	2.84	39.23	3.38	50.65
1:11:22 PM	17.84	36.46	20.52	48.87
2:11:22 PM	32.84	30.21	35.26	44.88
3:11:22 PM	47.84	21.43	47.11	39.31
4:11:22 PM	62.84	10.98	56.49	32.82
5:11:22 PM	77.84	-0.57	64.08	25.92
6:11:22 PM	92.84	-12.83	70.46	19.04

July				
Local Latitude (N)	**Local Longitude (E)**	**Standard Longitude (E)**	**Declination angle, δ (degrees)**	**hss; hsr=-hss**
-27.6154	152.7596	150	21.10	78.54
Day Hour AST	**Solar Hour Angle, *h***	**Solar Altitude Angle, α**	**Solar Azimuth Angle, *z***	**Incidence angle, θ**
5:05:39 AM	-103.59	-21.17	-76.52	12.56
6:05:39 AM	-88.59	-8.42	-70.53	19.25
7:05:39 AM	-73.59	3.82	-63.76	26.18
8:05:39 AM	-58.59	15.31	-55.64	32.98
9:05:39 AM	-43.59	25.59	-45.49	39.22
10:05:39 AM	-28.59	33.99	-32.57	44.33
11:05:39 AM	-13.59	39.54	-16.51	47.68
12:05:39 PM	1.41	41.26	1.75	48.71
1:05:39 PM	16.41	38.76	19.76	47.21
2:05:39 PM	31.41	32.59	35.25	43.48
3:05:39 PM	46.41	23.77	47.59	38.11
4:05:39 PM	61.41	13.22	57.30	31.73
5:05:39 PM	76.41	1.57	65.12	24.87
6:05:39 PM	91.41	-10.79	71.71	17.96

Aug				
Local Latitude (N)	**Local Longitude (E)**	**Standard Longitude (E)**	**Declination angle, δ (degrees)**	**hss; hsr=-hss**
-27.6154	152.7596	150	13.30	83.01
Day Hour AST	**Solar Hour Angle, *h***	**Solar Altitude Angle, *α***	**Solar Azimuth Angle, *z***	**Incidence angle, θ**
5:07:40 AM	-103.08	-17.57	-83.88	5.84
6:07:40 AM	-88.08	-4.46	-77.32	12.64
7:07:40 AM	-73.08	8.30	-70.21	19.58
8:07:40 AM	-58.08	20.44	-61.84	26.25
9:07:40 AM	-43.08	31.55	-51.26	32.23
10:07:40 AM	-28.08	40.86	-37.28	37.00
11:07:40 AM	-13.08	47.17	-18.91	40.03
12:07:40 PM	1.92	49.05	2.85	40.89
1:07:40 PM	16.92	45.92	24.02	39.45
2:07:40 PM	31.92	38.71	41.25	35.92
3:07:40 PM	46.92	28.84	54.24	30.79
4:07:40 PM	61.92	17.42	64.14	24.59
5:07:40 PM	76.92	5.08	72.12	17.81
6:07:40 PM	91.92	-7.78	79.02	10.88

September				
Local Latitude (N)	**Local Longitude (E)**	**Standard Longitude (E)**	**Declination angle, δ (degrees)**	**hss; hsr=-hss**
-27.6154	152.7596	150	1.99	88.97
Day Hour AST	**Solar Hour Angle, *h***	**Solar Altitude Angle, *α***	**Solar Azimuth Angle, *z***	**Incidence angle, θ**
5:16:46 AM	-100.81	-10.50	-86.73	3.21
6:16:46 AM	-85.81	2.79	-86.29	3.71
7:16:46 AM	-70.81	15.96	-79.02	10.55
8:16:46 AM	-55.81	28.78	-70.60	16.93
9:16:46 AM	-40.81	40.85	-59.71	22.42
10:16:46 AM	-25.81	51.36	-44.17	26.61
11:16:46 AM	-10.81	58.62	-21.09	29.07
12:16:46 PM	4.19	60.12	8.43	29.53
1:16:46 PM	19.19	55.11	35.05	27.93
2:16:46 PM	34.19	45.75	53.60	24.46
3:16:46 PM	49.19	34.24	66.20	19.49
4:16:46 PM	64.19	21.68	75.51	13.44
5:16:46 PM	79.19	8.62	83.16	6.76
6:16:46 PM	94.19	-4.64	89.83	0.17

Oct				
Local Latitude (N)	**Local Longitude (E)**	**Standard Longitude (E)**	**Declination angle, δ (degrees)**	**hss; hsr=-hss**
-27.6154	152.7596	150	-10.04	95.23
Day Hour AST	**Solar Hour Angle, *h***	**Solar Altitude Angle, *α***	**Solar Azimuth Angle, *z***	**Incidence angle, θ**
5:25:31 AM	-98.62	-2.87	-77.11	12.88
6:25:31 AM	-83.62	10.24	-83.95	5.95
7:25:31 AM	-68.62	23.51	-89.25	0.69
8:25:31 AM	-53.62	36.75	-81.65	6.68
9:25:31 AM	-38.62	49.68	-71.79	11.67
10:25:31 AM	-23.62	61.67	-56.24	15.29
11:25:31 AM	-8.62	70.64	-26.44	17.27
12:25:31 PM	6.38	71.42	20.09	17.41
1:25:31 PM	21.38	63.29	52.99	15.70
2:25:31 PM	36.38	51.56	69.96	12.30
3:25:31 PM	51.38	38.71	80.37	7.50
4:25:31 PM	66.38	25.49	88.19	1.63
5:25:31 PM	81.38	12.21	84.95	4.93
6:25:31 PM	96.38	-0.93	78.16	11.84

Nov				
Local Latitude (N)	**Local Longitude (E)**	**Standard Longitude (E)**	**Declination angle, δ (degrees)**	**hss; hsr=-hss**
-27.6154	152.7596	150	-19.28	100.37
Day Hour AST	**Solar Hour Angle, *h***	**Solar Altitude Angle, *α***	**Solar Azimuth Angle, *z***	**Incidence angle, θ**
5:25:23 AM	-98.65	1.56	-68.99	21.00
6:25:23 AM	-83.65	14.21	-75.41	14.13
7:25:23 AM	-68.65	27.22	-81.38	7.66
8:25:23 AM	-53.65	40.45	-87.50	1.90
9:25:23 AM	-38.65	53.73	-85.23	2.82
10:25:23 AM	-23.65	66.80	-74.04	6.22
11:25:23 AM	-8.65	78.49	-45.40	8.05
12:25:23 PM	6.35	79.83	36.24	8.18
1:25:23 PM	21.35	68.76	71.49	6.61
2:25:23 PM	36.35	55.76	83.89	3.44
3:25:23 PM	51.35	42.49	88.51	1.10
4:25:23 PM	66.35	29.25	82.30	6.72
5:25:23 PM	81.35	16.19	76.35	13.10
6:25:23 PM	96.35	3.47	70.03	19.93

December				
Local Latitude (N)	**Local Longitude (E)**	**Standard Longitude (E)**	**Declination angle, δ (degrees)**	**hss; hsr=-hss**
-27.6154	152.7596	150	-23.12	102.70
Day Hour AST	**Solar Hour Angle, *h***	**Solar Altitude Angle, *α***	**Solar Azimuth Angle, *z***	**Incidence angle, θ**
5:16:54 AM	-100.78	1.70	-64.67	25.32
6:16:54 AM	-85.78	14.01	-70.96	18.46
7:16:54 AM	-70.78	26.77	-76.55	11.98
8:16:54 AM	-55.78	39.82	-81.90	6.21
9:16:54 AM	-40.78	53.05	-87.60	1.44
10:16:54 AM	-25.78	66.33	-84.87	2.06
11:16:54 AM	-10.78	79.28	-67.62	4.06
12:16:54 PM	4.23	84.11	41.29	4.42
1:16:54 PM	19.23	72.08	79.79	3.13
2:16:54 PM	34.23	58.85	89.50	0.26
3:16:54 PM	49.23	45.58	84.29	3.99
4:16:54 PM	64.23	32.44	78.89	9.36
5:16:54 PM	79.23	19.54	73.46	15.56
6:16:54 PM	94.23	0.00	66.51	23.49

Averaged Radiation Data

Jan Tracked Collector		
Hour LST	**G_Bn, W/m^2**	**Gbt, W/m^2**
6.00	0.00	0.00
7.00	333.81	326.96
8.00	602.39	599.52
9.00	658.03	658.01
10.00	676.74	675.52
11.00	654.00	650.55
12.00	497.19	493.80
13.00	485.81	483.31
14.00	492.94	492.13
15.00	490.23	490.19
16.00	469.55	467.08
17.00	421.94	412.80
18.00	238.45	225.98
19.00	0.00	0.00

Feb Tracked Collector		
Hour	**G_Bn, W/m^2**	**Gbt, W/m^2**
6.00	0.00	0.00
7.00	231.87	225.49
8.00	424.87	408.63
9.00	460.93	435.26
10.00	477.63	441.96
11.00	479.50	436.61
12.00	416.10	376.42
13.00	416.17	378.50
14.00	404.23	373.33
15.00	430.27	405.47
16.00	411.17	394.83
17.00	357.33	347.28
18.00	217.63	211.86
19.00	0.00	0.00

March Tracked Collector		
Hour	**G_Bn, W/m^2**	**Gbt, W/m^2**
6.00	0.00	0.00
7.00	237.32	236.44
8.00	486.00	476.41
9.00	589.74	563.85
10.00	588.42	547.61
11.00	621.81	566.77
12.00	565.32	511.41
13.00	568.68	518.81
14.00	564.03	525.70
15.00	565.19	541.24
16.00	558.13	547.79
17.00	447.74	446.32
18.00	199.45	199.29
19.00	0.00	0.00

Apr Tracked Collector		
Hour	**G_Bn, W/m^2**	**Gbt, W/m^2**
7.00	0.00	0.00
8.00	318.37	292.84
9.00	588.20	514.82
10.00	624.63	520.86
11.00	630.27	507.66
12.00	628.77	501.66
13.00	627.60	510.37
14.00	622.87	527.65
15.00	632.83	563.69
16.00	594.27	555.19
17.00	311.00	301.57
18.00	0.00	0.00

May Tracked Collector		
Hour	**G_Bn, W/m^2**	**Gbt, W/m^2**
7.00	0.00	0.00
8.00	287.77	244.37
9.00	455.94	359.69
10.00	498.45	366.17
11.00	518.19	361.92
12.00	507.29	350.15
13.00	525.65	374.54
14.00	558.13	423.50
15.00	577.03	471.64
16.00	512.58	449.36
17.00	318.68	295.71
18.00	0.00	0.00

June Tracked Collector		
Hour	**G_Bn, W/m^2**	**Gbt, W/m^2**
7.00	0.00	0.00
8.00	201.67	164.48
9.00	381.17	285.20
10.00	476.50	327.31
11.00	473.17	305.19
12.00	474.13	300.66
13.00	518.60	341.10
14.00	536.80	380.38
15.00	528.87	409.19
16.00	502.43	422.25
17.00	307.13	276.24
18.00	0.00	0.00

July Tracked Collector		
Hour	**G_Bn, W/m^2**	**Gbt, W/m^2**
7.00	0.00	0.00
8.00	322.90	270.86
9.00	486.77	377.14
10.00	552.55	395.28
11.00	579.03	389.87
12.00	597.52	394.32
13.00	595.32	404.42
14.00	580.39	421.15
15.00	547.29	430.63
16.00	497.58	423.20
17.00	337.13	305.86
18.00	0.00	0.00

Aug Tracked Collector		
Hour	**G_Bn, W/m^2**	**Gbt, W/m^2**
7.00	0.00	0.00
8.00	249.42	223.70
9.00	453.55	383.68
10.00	498.58	398.20
11.00	505.94	387.40
12.00	516.48	390.43
13.00	517.74	399.80
14.00	514.10	416.32
15.00	494.29	424.61
16.00	439.58	399.71
17.00	242.03	230.43
18.00	0.00	0.00

Sept Tracked Collector		
Hour	**G_Bn, W/m^2**	**Gbt, W/m^2**
6.00	0.00	0.00
7.00	64.27	63.18
8.00	358.63	343.10
9.00	565.10	522.37
10.00	593.27	530.44
11.00	608.57	531.91
12.00	601.70	523.55
13.00	614.80	543.21
14.00	593.13	539.91
15.00	586.93	553.32
16.00	568.10	552.53
17.00	364.53	362.00
18.00	72.90	72.90
19.00	0.00	0.00

Oct Tracked Collector		
Hour	**G_Bn, W/m^2**	**Gbt, W/m^2**
6.00	0.00	0.00
7.00	318.10	318.07
8.00	528.26	524.67
9.00	587.71	575.57
10.00	602.77	581.43
11.00	575.32	549.39
12.00	472.68	451.02
13.00	473.16	455.51
14.00	506.97	495.33
15.00	475.29	471.23
16.00	466.42	466.23
17.00	425.32	423.75
18.00	245.39	240.17
19.00	0.00	0.00
20.00	0.00	0.00

Nov Tracked Collector		
Hour	**G_Bn, W/m^2**	**Gbt, W/m^2**
6.00	0.00	0.00
7.00	251.33	249.09
8.00	462.90	462.65
9.00	517.70	517.07
10.00	523.13	520.06
11.00	512.57	507.51
12.00	455.90	451.26
13.00	445.43	442.48
14.00	455.73	454.91
15.00	462.80	462.71
16.00	463.57	460.39
17.00	436.63	425.27
18.00	255.77	240.45
19.00	0.00	0.00

Dec Tracked Collector		
Hour	**G_Bn, W/m^2**	**Gbt, W/m^2**
6.00	0.00	0.00
7.00	279.61	273.52
8.00	497.61	494.69
9.00	523.42	523.25
10.00	541.74	541.39
11.00	542.16	540.80
12.00	443.00	441.68
13.00	445.94	445.27
14.00	458.16	458.16
15.00	464.48	463.36
16.00	465.84	459.64
17.00	412.74	397.61
18.00	261.45	239.79
19.00	0.00	0.00

Monthly Collector Yield Results

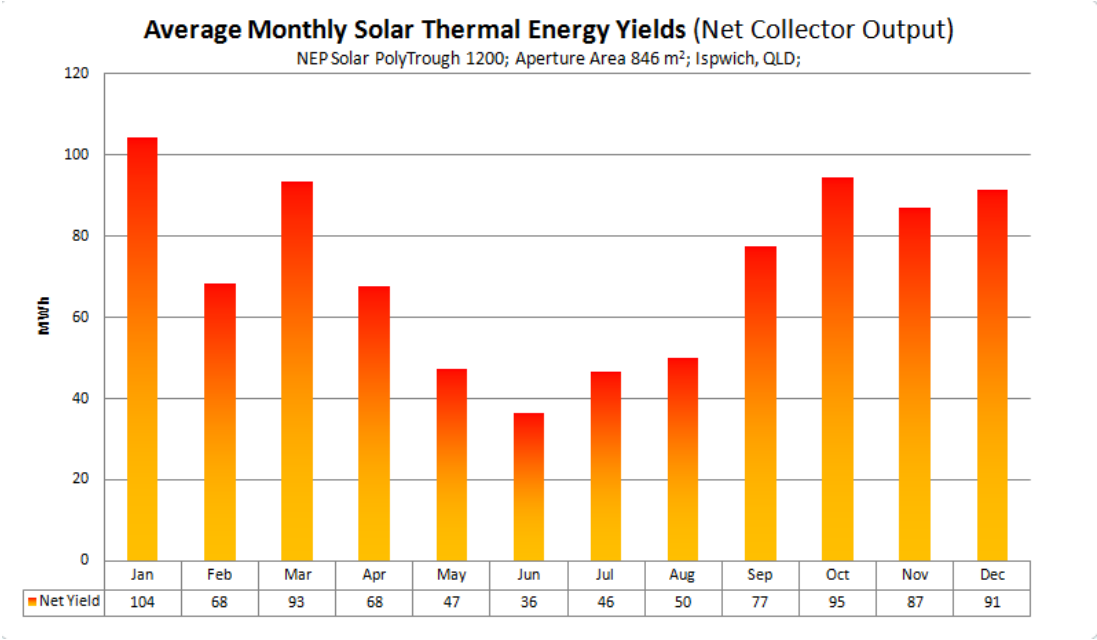

PolyTrough 1200; Field; January Average Day						
hour	**Gbt w/m^2**	**Incidence Angle**	**IAM, K_θ**	**Thermal Efficiency**	**Useful energy, Qu kJ**	**Power, kW**
6	0.00	18.27	0.93	0.0000	0.00	0.00
7	326.96	11.63	0.97	0.6437	635501.08	176.53
8	599.52	5.59	0.99	0.6622	1225956.62	340.54
9	658.01	0.47	1.00	0.6642	1362606.47	378.50
10	675.52	3.44	1.00	0.6648	1393607.55	387.11
11	650.55	5.89	0.99	0.6640	1332705.13	370.20
12	493.80	6.70	0.99	0.6575	999302.57	277.58
13	483.31	5.81	0.99	0.6569	979756.24	272.15
14	492.13	3.28	1.00	0.6574	1004341.78	278.98
15	490.19	0.70	1.00	0.6573	1004215.21	278.95
16	467.08	5.87	0.99	0.6559	945295.42	262.58
17	412.80	11.95	0.97	0.6522	811684.82	225.47
18	225.98	18.61	0.93	0.6254	409331.26	113.70
19	0.00	0.00	1.00	0.0000	0.00	0.00
				Total, kJ	12104304.15	
				Energy kWh	3362.31	

PolyTrough 1200; Field; Febuary Average Day						
hour	**Gbt w/m^2**	**Incidence Angle**	**IAM, K_θ**	**Thermal Efficiency**	**Useful energy, Qu kJ**	**Power, kW**
6	0.00	13.34	0.96	0.0000	0.00	0.00
7	231.87	13.46	0.96	0.6269	434907.63	120.81
8	424.87	15.89	0.95	0.6531	818546.07	227.37
9	460.93	19.21	0.93	0.6556	871241.36	242.01
10	477.63	22.29	0.90	0.6566	881851.06	244.96
11	479.50	24.42	0.89	0.6567	868147.99	241.15
12	416.10	25.22	0.88	0.6524	742551.33	206.26
13	416.17	24.56	0.89	0.6524	747565.61	207.66
14	404.23	22.55	0.90	0.6515	738837.25	205.23
15	430.27	19.55	0.92	0.6535	808670.58	224.63
16	411.17	16.21	0.95	0.6520	789311.91	219.25
17	357.33	13.62	0.96	0.6472	691259.47	192.02
18	217.63	13.22	0.96	0.6232	406277.20	112.85
19	0.00	0.00	1.00	0.0000	0.00	0.00
				Total, kJ	8799167.48	
				Power kWh	2444.21	

PolyTrough 1200; Field; March Average Day						
hour	**Gbt w/m^2**	**Incidence Angle**	**IAM, K_θ**	**Thermal Efficiency**	**Useful energy, Qu kJ**	**Power kW**
6	0.00	1.91	1.00	0.0000	0.00	0.00
7	236.44	4.95	0.99	0.6281	459278.15	127.58
8	476.41	11.40	0.97	0.6565	945414.69	262.62
9	563.85	17.04	0.94	0.6608	1091069.04	303.07
10	547.61	21.46	0.91	0.6601	1023781.88	284.38
11	566.77	24.29	0.89	0.6610	1034175.58	287.27
12	511.41	25.23	0.88	0.6584	920996.28	255.83
13	518.81	24.17	0.89	0.6588	944594.74	262.39
14	525.70	21.25	0.91	0.6591	983089.12	273.08
15	541.24	16.74	0.94	0.6599	1047821.60	291.06
16	547.79	11.04	0.97	0.6601	1094912.31	304.14
17	446.32	4.56	1.00	0.6546	904502.58	251.25
18	199.29	2.32	1.00	0.6175	382709.98	106.31
19	0.00	0.00	1.00	0.0000	0.00	0.00
				Total, kJ	10832345.95	
				Power kWh	3008.98	

PolyTrough 1200; Field; April Average Day						
hour	**Gbt w/m^2**	**Incidence Angle**	**IAM, K_θ**	**Thermal Efficiency**	**Useful energy, Qu kJ**	**Power kW**
7	0.00	16.51	0.94	0.0000	0.00	0.00
8	292.84	23.10	0.90	0.6389	522314.80	145.09
9	514.82	28.92	0.84	0.6586	890511.54	247.36
10	520.86	33.50	0.80	0.6589	848799.27	235.78
11	507.66	36.34	0.76	0.6582	791245.74	219.79
12	501.66	37.08	0.75	0.6579	772142.14	214.48
13	510.37	35.59	0.77	0.6584	805308.29	223.70
14	527.65	32.10	0.81	0.6592	877414.34	243.73
15	563.69	27.03	0.86	0.6608	999687.94	277.69
16	555.19	20.90	0.91	0.6605	1043377.33	289.83
17	301.57	14.15	0.96	0.6402	575476.78	159.85
18	0.00	7.21	0.99	0.0000	0.00	0.00
				Total, kJ	8126278.19	
				Power kWh	2257.30	

PolyTrough 1200; Field; May Average Day						
hour	**Gbt w/m^2**	**Incidence Angle**	**IAM, K_θ**	**Thermal Efficiency**	**Useful energy, Qu kJ**	**Power kW**
7	0.00	25.16	0.88	0.0000	0.00	0.00
8	244.37	31.88	0.81	0.6299	389431.50	108.18
9	359.69	37.92	0.74	0.6474	537040.21	149.18
10	366.17	42.73	0.68	0.6481	498898.49	138.58
11	361.92	45.70	0.63	0.6476	460568.05	127.94
12	350.15	46.35	0.62	0.6464	437661.51	121.57
13	374.54	44.56	0.65	0.6489	490602.73	136.28
14	423.50	40.64	0.71	0.6530	606572.22	168.49
15	471.64	35.18	0.78	0.6562	746541.73	207.37
16	449.36	28.76	0.85	0.6548	774343.81	215.10
17	295.71	21.89	0.91	0.6394	533512.03	148.20
18	0.00	14.98	0.95	0.0000	0.00	0.00
				Total, kJ	5475172.28	
				Power kWh	1520.88	

PolyTrough 1200; Field; June Average Day						
hour	**Gbt w/m^2**	**Incidence Angle**	**IAM, K_θ**	**Thermal Efficiency**	**Useful energy, Qu kJ**	**Power kW**
7	0.00	28.55	0.85	0.0000	0.00	0.00
8	164.48	35.35	0.77	0.6034	238742.03	66.32
9	285.20	41.56	0.69	0.6377	391716.39	108.81
10	327.31	46.61	0.62	0.6437	404758.17	112.43
11	305.19	49.84	0.57	0.6408	344084.74	95.58
12	300.66	50.65	0.55	0.6401	330507.81	91.81
13	341.10	48.87	0.58	0.6454	398198.77	110.61
14	380.38	44.88	0.64	0.6494	494995.57	137.50
15	409.19	39.31	0.72	0.6519	600025.83	166.67
16	422.25	32.82	0.80	0.6529	688529.86	191.26
17	276.24	25.92	0.87	0.6362	477263.66	132.57
18	0.00	19.04	0.93	0.0000	0.00	0.00
				Total, kJ	4368822.83	
				Power kWh	1213.56	

PolyTrough 1200; Field; July Average Day						
hour	**Gbt w/m^2**	**Incidence Angle**	**IAM, K_θ**	**Thermal Efficiency**	**Useful energy, Qu kJ**	**Power kW**
7	0.00	26.18	0.87	0.0000	0.00	0.00
8	270.86	32.98	0.80	0.6352	428717.36	119.09
9	377.14	39.22	0.72	0.6491	551641.81	153.23
10	395.28	44.33	0.65	0.6507	522048.48	145.01
11	389.87	47.68	0.60	0.6503	473799.32	131.61
12	394.32	48.71	0.58	0.6507	466263.08	129.52
13	404.42	47.21	0.61	0.6515	498488.04	138.47
14	421.15	43.48	0.67	0.6528	568683.18	157.97
15	430.63	38.11	0.74	0.6535	646832.29	179.68
16	423.20	31.73	0.82	0.6530	700524.12	194.59
17	305.86	24.87	0.88	0.6409	538035.34	149.45
18	0.00	17.96	0.94	0.0000	0.00	0.00
				Total, kJ	5395033.01	
				Power kWh	1498.62	

PolyTrough 1200; Field; Aug Average Day						
hour	**Gbt w/m^2**	**Incidence Angle**	**IAM, K_θ**	**Thermal Efficiency**	**Useful energy, Qu kJ**	**Power kW**
7	0.00	19.58	0.92	0.0000	0.00	0.00
8	223.70	26.25	0.87	0.6248	378294.26	105.08
9	383.68	32.23	0.81	0.6497	627725.43	174.37
10	398.20	37.00	0.75	0.6510	607245.44	168.68
11	387.40	40.03	0.71	0.6501	558926.10	155.26
12	390.43	40.89	0.70	0.6503	554214.22	153.95
13	399.80	39.45	0.72	0.6511	584101.41	162.25
14	416.32	35.92	0.77	0.6525	647575.20	179.88
15	424.61	30.79	0.83	0.6531	711694.91	197.69
16	399.71	24.59	0.88	0.6511	716356.43	198.99
17	230.43	17.81	0.94	0.6266	420549.05	116.82
18	0.00	10.88	0.97	0.0000	0.00	0.00
				Total, kJ	5806682.45	
				Power kWh	1612.97	

PolyTrough 1200; Field; September Average Day						
hour	**Gbt w/m^2**	**Incidence Angle**	**IAM, K_θ**	**Thermal Efficiency**	**Useful energy, Qu kJ**	**Power kW**
6	0.00	3.71	1.00	0.0000	0.00	0.00
7	63.18	10.55	0.98	0.0000	0.00	0.00
8	343.10	16.93	0.94	0.6456	649080.68	180.30
9	522.37	22.42	0.90	0.6590	966782.89	268.55
10	530.44	26.61	0.87	0.6593	942961.44	261.93
11	531.91	29.07	0.84	0.6594	919649.28	255.46
12	523.55	29.53	0.84	0.6590	899653.26	249.90
13	543.21	27.93	0.85	0.6599	952540.37	264.59
14	539.91	24.46	0.89	0.6598	981803.27	272.72
15	553.32	19.49	0.93	0.6604	1051396.89	292.05
16	552.53	13.44	0.96	0.6604	1091717.59	303.25
17	362.00	6.76	0.99	0.6476	721475.06	200.41
18	72.8997	0.1740	1.003	0.5014	113985.63	31.66267
19	0.0000	0.0000	1.003	0.0000	0.00	0
				Total, kJ	9291046.36	
				Power kWh	2580.85	

PolyTrough 1200; Field; Oct Average Day						
hour	**Gbt w/m^2**	**Incidence Angle**	**IAM, K_θ**	**Thermal Efficiency**	**Useful energy, Qu kJ**	**Power kW**
6.00	0.00	5.95	0.99	0.0000	0.00	0.00
7.00	318.07	0.69	1.00	0.6425	637013.86	176.95
8.00	524.67	6.68	0.99	0.6591	1064409.92	295.67
9.00	575.57	11.67	0.97	0.6613	1149174.17	319.22
10.00	581.43	15.29	0.95	0.6616	1138845.93	316.35
11.00	549.39	17.27	0.94	0.6602	1060435.53	294.57
12.00	451.02	17.41	0.94	0.6549	862767.56	239.66
13.00	455.51	15.70	0.95	0.6552	881458.47	244.85
14.00	495.33	12.30	0.97	0.6576	980313.37	272.31
15.00	471.23	7.50	0.99	0.6562	949319.65	263.70
16.00	466.23	1.63	1.00	0.6559	951958.70	264.43
17.00	423.75	4.93	0.99	0.6530	855882.00	237.75
18	240.17	11.84	0.97	0.63	455656.68	126.57
19	0.00	0.00	1.00	0.00	0.00	0.00
				Total, kJ	10987235.84	
				Power kWh	3052.01	

PolyTrough 1200; Field; Nov Average Day						
hour	**Gbt w/m^2**	**Incidence Angle**	**IAM, K_θ**	**Thermal Efficiency**	**Useful energy, Qu kJ**	**Power kW**
6	0.00	14.13	0.96	0.0000	0.00	0.00
7	249.09	7.66	0.99	0.6309	482235.57	133.95
8	462.65	1.90	1.00	0.6557	943942.88	262.21
9	517.07	2.82	1.00	0.6587	1058265.59	293.96
10	520.06	6.22	0.99	0.6588	1056137.97	293.37
11	507.51	8.05	0.99	0.6582	1023636.77	284.34
12	451.26	8.18	0.98	0.6549	905206.97	251.45
13	442.48	6.61	0.99	0.6543	891418.72	247.62
14	454.91	3.44	1.00	0.6552	924976.03	256.94
15	462.71	1.10	1.00	0.6557	945142.39	262.54
16	460.39	6.72	0.99	0.6555	928849.24	258.01
17	425.27	13.10	0.96	0.6531	832583.12	231.27
18	240.45	19.93	0.92	0.63	433688.46	120.47
19	0.00	0.00	1.00	0.00	0.00	0.00
				Total, kJ	10426083.72	
				Power kWh	2896.13	

PolyTrough 1200; Field; December Average Day						
Hour	**Gbt w/m^2**	**Incidence Angle**	**IAM, K_θ**	**Thermal Efficiency**	**Useful energy, Qu kJ**	**Power kW**
6	0.00	18.46	0.93	0.0000	0.00	0.00
7	273.52	11.98	0.97	0.6357	524154.89	145.60
8	494.69	6.21	0.99	0.6575	1002624.34	278.51
9	523.25	1.44	1.00	0.6590	1073756.75	298.27
10	541.39	2.06	1.00	0.6599	1111420.01	308.73
11	540.80	4.06	1.00	0.6598	1105981.10	307.22
12	441.68	4.42	1.00	0.6543	894946.31	248.60
13	445.27	3.13	1.00	0.6545	905040.68	251.40
14	458.16	0.26	1.00	0.6554	936313.24	260.09
15	463.36	3.99	1.00	0.6557	941819.02	261.62
16	459.64	9.36	0.98	0.6555	918726.55	255.20
17	397.61	15.56	0.95	0.6509	765056.59	212.52
18.00	239.79	23.49	0.89	0.63	419450.73	116.51
19.00	0.00	0.00	1.00	0.00	0.00	0.00
				Total, kJ	10599290.20	
				Power kWh	2944.25	

NEPSOLAR

NEP Solar PolyTrough 1200
Design data and thermal performance

Simulated thermal performance and dimensions of NEP Solar PolyTrough collecor field for process heat applications.

Real performance depends on the specific project location and characteristics. Performance figures are for feasibility study phase and budgeting only.

General Field Data

Project:	Ipswich Solar Cooling, Zach Muller	
Location:	Ipsqich, Australia	
Latitude:	-28	° North
Solar radiation:	1,913	kWh/m2.year DNI
Radiation data site:	Ipswich - Australia	
Collector axis orientation:	0	° from North-South orientation
Number of PolyTrough 1200 modules:	30	at 28.8 m2 per module
Number of rows x modules per row:	15 x 2	
Aperture area (active collector area):	864	m2
Ground- or roof area:	2,400	m2
Total field length x width:	50 x 48	m
Distance to plant room:	50	m
Heat transfer medium:	Water	
Design temperature difference:	30	degC
Operating pressure:	16	bar
Design storage time:	-	hour
Storage tank size:	-	m3
Supply/Return piping size:	-	DN

Performance at design conditions

Design solar radiation (DNI)	1000	W/m2 DNI
Design supply temperature:	180	deg C
Design field thermal power:	**518**	**kW**

Annual yield

Assumption: All solar generated heat can be used (no heat dump or collector defocusing)
Net yield includes availability and field losses

Net specific yield:	770	kWh/m2/year
Net annual yield:	**665**	**MWh/year**
Fossil fuel savings	831	MWh/year (for 80% boiler efficiency)
CO2 displaced	220	tons CO2/year (Oil)

Dimensions (all dimensions in metres)

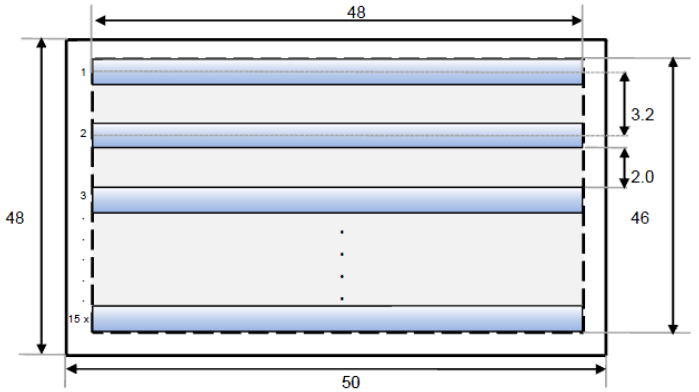

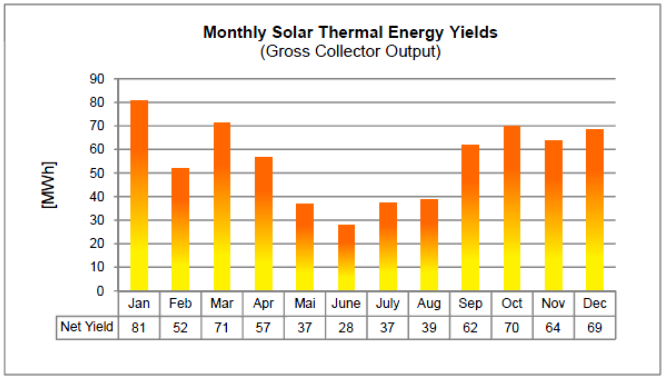

Zach Muller

University of Southern Queensland
Faculty of Engineering and Surveying

NEPSOLAR

NEP Solar PolyTrough 1200
Design data and thermal performance

Simulated thermal performance and dimensions of NEP Solar PolyTrough collecor field for process heat applications.

Real performance depends on the specific project location and characteristics. Performance figures are for feasibility study phase and budgeting only.

General Field Data

Project:	Ipswich Solar Cooling, Zach Muller	
Location:	Ipsqich, Australia	
Latitude:	-27.61	° North
Solar radiation:	1,913	kWh/m2.year DNI
Radiation data site:	Ipswich - Australia	
Collector axis orientation:	0	° from North-South orientation
Number of PolyTrough 1200 modules:	30	at 28.8 m2 per module
Number of rows x modules per row:	15 x 2	
Aperture area (active collector area):	864	m2
Ground- or roof area:	2,400	m2
Total field length x width:	50 x 48	m
Distance to plant room:	50	m
Heat transfer medium:	Water	
Design temperature difference:	30	degC
Operating pressure:	16	bar
Design storage time:	-	hour
Storage tank size:	-	m3
Supply/Return piping size:	65	DN

Performance at design conditions

Design solar radiation (DNI)	1000	W/m2 DNI
Design supply temperature:	180	deg C
Design field thermal power:	**518**	**kW**

Annual yield

Assumption: All solar generated heat can be used (no heat dump or collector defocusing)
Net yield includes availability and field losses

Net specific yield:	770	kWh/m2/year
Net annual yield:	**665**	**MWh/year**
Fossil fuel savings	831	MWh/year (for 80% boiler efficiency)
CO2 displaced	220	tons CO2/year (Oil)

Performance Graphs

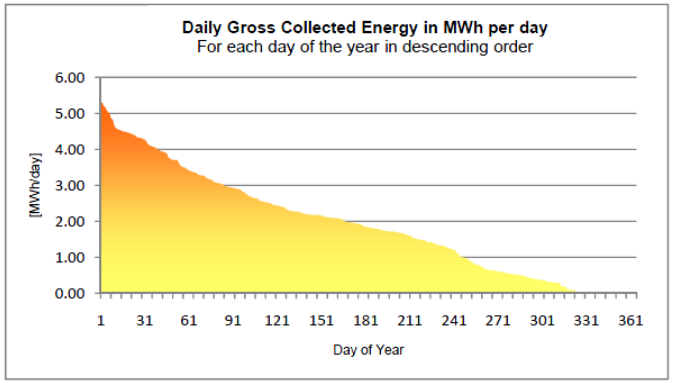

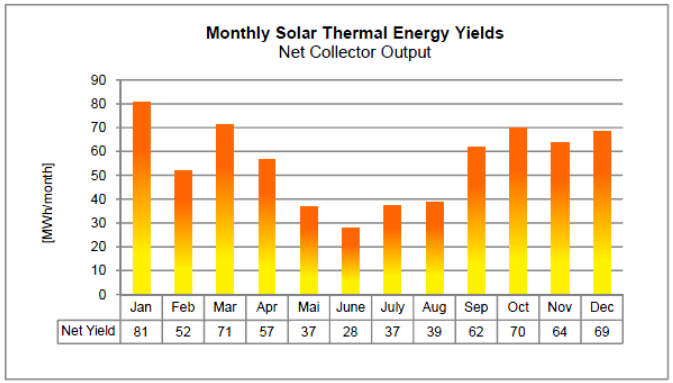

T

Appendix D – BROAD Absorption Chiller Data Sheets

11

Packaged Waste Heat Chiller (Hot Water Chiller) Performance Data

jacket water from generator and industrial waste hot water

(pump set, cooling tower, machine room's data as the same as DFA)

code	model	cooling capacity	chilled w.		cooling W.		hot water cons-umption	power demand	solution weight	unit ship. wt.	chiller ship. Wt.	unit operation weight
			flowrate	pressure drop	flowrate	pressure drop						
		kW	m^3/h	kPa	m^3/h	kPa	m^3/h	kW	t	t	t	t
two-stage hot water chiller BH hot water 180°C	20	233	28.5	30	48.8	50	10.3	1.7	0.98	3.3	/	4.7
	50	582	71.3	30	122	50	25.7	4.3	2.2	5.8	/	8.7
	75	872	107	30	183	50	38.5	4.6	2.8	7	5.4	11.1
	100	1163	142	30	244	50	51.4	6.8	3.4	9.3	7	13.7
	125	1454	178	30	305	50	64.2	6.8	4.4	10.7	8.3	16.1
	150	1745	214	40	366	50	77.1	6.8	4.9	11.9	9.2	18.6
	200	2326	285	40	488	50	103	10.2	7.1	15.2	12	24.7
	250	2908	356	50	610	60	128	10.2	7.8	19.3	14.5	31.6
	300	3489	427	50	733	60	154	11.7	10.6	21.5	16.3	36.7
	400	4652	570	50	977	60	206	13.2	12.1	/	21.3	46.6
	500	5815	712	60	1221	70	257	17.7	14.8	/	25.9	53.3
	600	6978	854	60	1465	70	308	20.7	18.1	/	29.9	64.7
	800	9304	1139	60	1953	70	411	25.9	24.2	/	38.3	81.4
	1000	11630	1429	60	2442	70	514	34.9	30.5	/	37.5	97.0
single-stage hot water chiller BDH hot water 98°C	20	205	25.1	25	61.7	50	23.2	2.5	0.8	2.9	/	3.8
	50	512	62.7	25	154	50	57.9	2.5	1.65	4.9	/	7.0
	75	767	93.9	25	231	60	86.8	5.3	2.15	6.3	/	9.3
	100	1023	125	25	308	60	116	5.7	2.42	8.0	/	11.5
	125	1279	157	25	385	60	145	5.7	3.2	9.4	/	14.4
	150	1535	188	30	462	60	174	5.7	3.52	10.8	/	16.1
	200	2046	251	30	616	70	232	8.6	5.5	14.5	/	22.3
	250	2558	313	40	771	70	289	10.1	6.0	17.7	/	26.1
	300	3069	376	40	925	70	347	10.1	8.25	19.8	/	30.5
	400	4092	501	40	1233	70	463	13.9	8.92	26.3	/	39.8
	500	5115	626	50	1541	90	579	13.8	11.7	30.8	/	48.3
	600	6138	752	50	1849	90	695	17.5	14.5	36.3	/	56.5
	800	8184	1002	50	2466	90	926	27.3	19.7	45.8	/	75.5
	1000	10230	1253	50	3082	100	1158	27.3	24.1	46.5	/	82.8 P

General Conditions:

1. Rated hot W. inlet/outlet temp.:
   Two-stage hot W. chiller:180°C/165°C
   Single-stage hot W. chiller: 98°C/88°C
2. Rated chilled W. outlet/inlet temp.: 7°C/14°C
3. Rated cooling W. outlet/inlet temp.: 37°C/30°C
4. Lowest permitted outlet temperature for chilled water: 5°C (except special order)
5. Lowest permitted inlet temperature for cooling water: 10°C
6. Adjustable chilled water flowrate: 50%~120%
7. pressure limit for chilled/cooling W.:0.8mpa
8. Adjustable load: 5%~115%
9. Fouling factor for chilled W., cooling W.,:0.086 m2·K/kW
10. LiBr Solution concentration: 52%
11. Machine room temperature: 5~43°C,humidity≤85%
12. Rated COP:two-stage hot W. chiller:1.41
    single-stage hot W. chiller:0.76
13. Designed lifespan: 25 years

Note: 1. Pumpset price for packaged single-stage hot W. chiller is 28%

Model Selection Curves

(chilled/cooling water temp, cooling capacity, COP) orange means the rated value

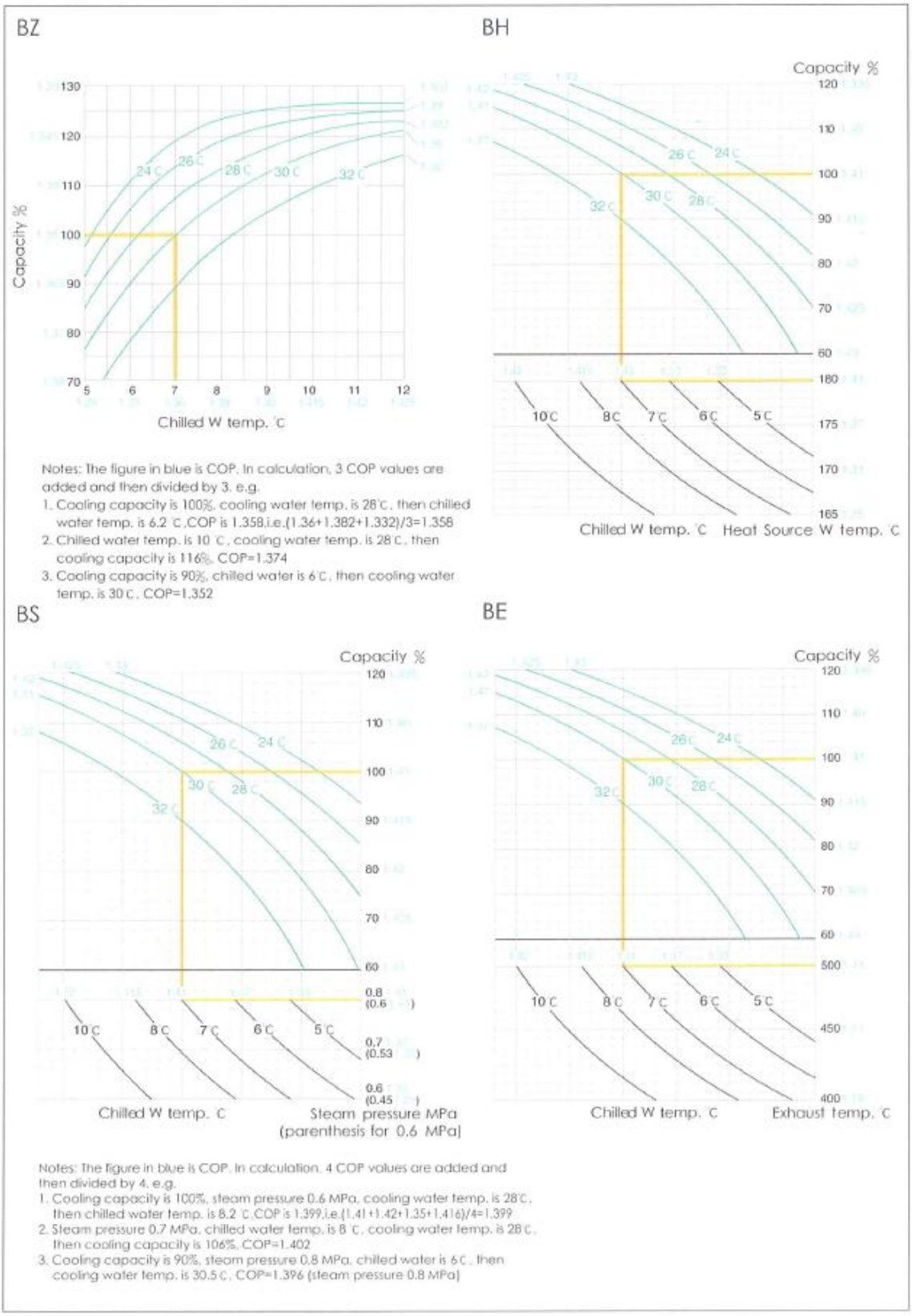

Note that the image is a little unclear. It was provided this way.

Appendix E – Psychometric Chart